

DESIGN OF AN ADJUSTABLE GRAVITY EQUILIBRATOR USING TORSION BARS

Freeke J.C. van Osch, Just L. Herder

Faculty of Mechanical, Maritime and Materials Engineering

Department of BioMechanical Engineering

Delft University of Technology

Delft, The Netherlands

Email: f.j.c.vanosch@student.tudelft.nl

ABSTRACT

Static balancing is a useful concept to reduce operating effort in mechanisms. A statically balanced system which is designed to counterbalance a mass, is referred to as a gravity equilibrator. The potential energy in a gravity equilibrator is constant, which is achieved by mechanical springs in most of the times. Enabling spring parameter adjustment is desirable to make the system suitable for different masses. Often helical springs are used, which have the problem that they take a lot of space within the workspace of the mechanism. The goal of this paper is to develop an adjustable gravity equilibrator using torsion bars instead of helical springs, which saves space in the working area. Static balancing is achieved by a new Double-Cam Transmission (DCT). Adjustability is achieved by changing the active length of the torsion bars. A demonstrator was designed and it was shown that the system is in theory perfectly balanced, for different active lengths of the torsion bars. Our DCT design, and a general method to calculate its design parameters, are presented. The size of the DCT can be chosen arbitrarily. Adjustability is possible on a continuous, self-selected range of masses and energy-free when the torsion bars are not rotated.

INTRODUCTION

A gravity equilibrator is a statically balanced system which is designed to counterbalance a mass [1]. The principle of static balancing is that the system has a constant potential energy within a certain range of motion, which means that any preferred position is eliminated. Hardly no operating effort is needed to move the mass to a different position within this range. An external force is only needed to accelerate or decelerate the mass.

Constant potential energy of a system can be achieved by using counterweights or mechanical springs [2]. In many cases it

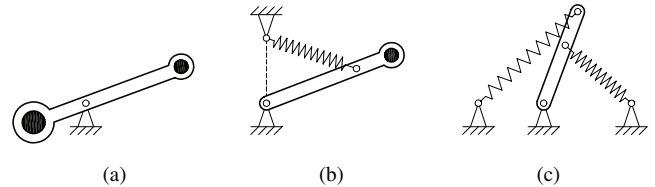


FIGURE 1. Similar static balancing principles: (a) mass-to-mass, (b) spring-to-mass and (c) spring-to-spring balancing [3]

is desirable to use mechanical springs instead of counterweights, since then the total weight of the system is reduced. Three similar static balancing principles may be distinguished: mass-to-mass balancing, spring-to-mass balancing and spring-to-spring balancing (see Fig. 1). This paper focuses on the principle of spring-to-mass balancing.

A disadvantage of the existing spring-to-mass balancers, is that the helical spring takes a lot of space within the workspace. However, when a torsion spring is used at the pivot point, the helical spring can be removed (see Fig. 2).

Several types of torsion springs exist. A type of torsion spring that does not take up a lot of workspace and stores a relatively large amount of potential energy, is the torsion bar [4].

An example of an existing product which counterbalances a mass and makes use of torsion bars is the HCI Foldable Container [5]. This container can be folded when it is empty, which saves space when it is transported or stored. However, this system is not perfectly statically balanced, since not every preferred position is eliminated [6]. A statically balanced system would be desirable though, to further reduce the operating effort.

A perfectly statically balanced system using torsion bars is not known by the authors. In many applications it is desirable to be able to adjust the gravity equilibrator for a different mass

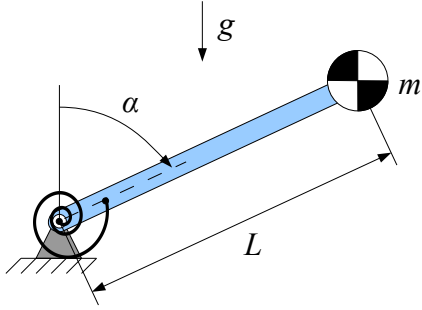


FIGURE 2. Spring-to-mass balancing with a torsion spring. The torsion spring is located at the pivot point, which saves space within the workspace of the mechanism.

as well [1]. An adjustable gravity equilibrator using torsion bars will bring new fields of application into existence.

For example, a case for a new application could be a TV dresser. Some TV dressers have the opportunity to hide the TV in the dresser when it is not used. Such a dresser should be higher than the height of the TV, which is seen as unaesthetic and uncomfortable. A solution to this problem is the DYNTEQ flatscreenlift [7]. The TV is stored in the dresser at an angle, so the height of the dresser can be decreased. A disadvantage of this design is that a lot of space is taken by the flatscreenlift and the TV. When the flatscreenlift is replaced by an adjustable gravity equilibrator with torsion bars, space in the dresser is saved. The mass in Fig. 2 is then replaced by a flat screen TV. This TV can be rotated from a vertical position to a horizontal position and vice versa. Since the system is statically balanced, hardly no operating effort is needed to rotate the TV. By making the system adjustable, different TVs can be balanced with the same system.

The goal of this paper is to develop a new theoretical perfectly balanced system, for counterbalancing different masses within a specified range, using torsion bars. This paper focuses on purely mechanical solutions.

The paper is structured as follows: first the method, including the design requirements, is explained. Subsequently the conceptual design is presented, which is followed up by a chapter on the final design. Finally the prototype and results are presented and discussed.

METHOD

In the basic gravity equilibrator, the moment M_{mass} exerted by the mass m on the pivot point (see Fig. 2), depending on the angle of rotation α , is:

$$M_{mass}(\alpha) = mgL \sin \alpha \quad (1)$$

where g is the gravity constant and L is the length of the lever.

The moment M_{bars} exerted by torsion bars with a solid circular cross section, depending on the angle of rotation β , is (adapted from [8,9]):

$$M_{bars}(\beta) = \underbrace{\frac{\pi}{32} G \frac{nd^4}{l}}_{k_c} (\beta + \beta_0) \quad (2)$$

where G is the shear modulus, n is the number of torsion bars placed in parallel, d is the diameter of the solid circular cross section, l is the active length of a torsion bar, k_c is the stiffness of torsion bars with a solid circular cross section and β_0 is the angle of rotation of the torsion bar(s) at starting position.

We want to achieve that:

$$M_{mass}(\alpha) = -M_{bars}(\beta) \quad \text{for } \alpha_{min} \leq \alpha \leq \alpha_{max} \quad (3)$$

Then the mass has no preferred position and thus the system is statically balanced within the range of α . For cases that can be modelled as an inverted pendulum as shown in Fig. 2, it holds that $M_{mass}(0) = 0$ and thus $M_{bars}(0) = 0$ Nm. This implies that $\beta_0 = 0$ rad, which simplifies Eqn. (2).

Design requirements

The design requirements are based on a specific case for M_{mass} . For this specific case we take the TV dresser with a 40/42 inch flat screen TV, which can be modelled as an inverted pendulum. The design requirements are summarized in Tab. 1.

- The first requirement involves the range of α . The TV is rotated from horizontal to vertical position and vice versa, thus $0 \leq \alpha \leq \frac{\pi}{2}$ rad.
- The second requirement involves the mass m to be balanced. In an adjustable system m can take more than just one value. The weight of a 40/42 inch flat screen TV is about 15 to 25 kg. The total mass of the system also includes the mass of the lever and the cover of the dresser. Therefore, for m we chose a range of $20 \leq m \leq 30$ kg.
- The third requirement involves the length L of the lever. The height of a 40/42 inch flat screen TV is about 600 mm. The centre of mass is assumed to be at a height of 300 mm. To have some space left to build in the torsion bars, we take $L = 400$ mm.
- The fourth requirement defines a parameter of $M_{bars}(\beta)$, which is the active length l of the torsion bar(s). The width of a 40/42 inch flat screen TV is about 1000 mm. Therefore we decide to restrict l and chose $l < 1000$ mm.

TABLE 1. Design requirements of the adjustable gravity equilibrator with torsion bars applied to the case of the TV dresser

Parameter	Symbol	Requirement
Angle of rotation of mass	α	$0 < \alpha < \frac{\pi}{2}$ rad
Mass	m	$20 < m < 30$ kg
Length of lever	L	$L = 400$ mm
Active length of torsion bar(s)	l	$l < 1000$ mm

CONCEPTUAL DESIGN

The development of the adjustable gravity equilibrator using torsion bars is split up into two sub problems. The first problem concerns the design of a perfectly statically balanced system and the second one concerns the design of a mechanism for an adjustable system.

Statically balanced system

For a statically balanced system we are looking for a relation for β , which depends on α , in such a way that Eqn. (3) holds. In other words, a specific transmission between α and β is needed. A non-constant transmission provides the opportunity to define a specific relation between two rotating axes [10–14]. A double-cam transmission (DCT) can be used, where two cams are needed which are connected to each other. We have chosen to connect the cams to each other with a cable, which is flexible and can be easily attached. The length of the cable is fixed, thus when one of the cams rotates, the other cam has to rotate as well. When the shapes of the cams are different, they will not rotate with the same angle of rotation and a specific relation between α and β can be determined.

Adjustable system

For an adjustable system we are looking for a way to change m and M_{bars} to the same extent, in such a way that Eqn. (3) holds. One possibility is to look at the variable β and another possibility is to look at the constant k_c .

A continuous variable transmission (CVT) provides the possibility to vary the transmission constant between α and β . For example, if we double the transmission constant, β rotates as twice as much, and a mass twice as big can be balanced. However, most of the times CVTs are big and complex systems [15–18]. Therefore, we first look at more convenient possibilities to change M_{bars} by changing k_c .

The parameters which concern k_c are n , d , G and l . Thus for a torsion bar of a specific material, we can either change n , d or l . The torsion bar diameter d can not be changed anymore when the system is in use. The only two parameters changeable when

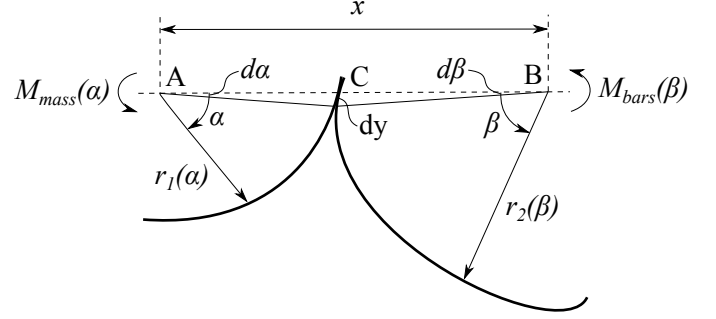


FIGURE 3. Schematic representation of a part of the circumference of the two cams (thick lines). The distance x between the centres of the cams is fixed by choosing A and B . The point of contact C of the two cams is always on the dashed horizontal line.

the system is in use, are n and l .

Since n is an integer value, for every different mass which is attached to the system, another torsion bar or combination of torsion bars is required [19]. In this way many torsion bars are needed, which should be activated or deactivated individually for each specific mass. Because the value of l is a continuous value, one can balance infinitely many different masses within a specific range. Even when more torsion bars are placed in parallel, it is possible to adapt l for all torsion bars at the same time [20]. To conclude, changing k_c by adapting l is the most convenient option.

FINAL DESIGN

The concept for a statically balanced system and the concept for an adjustable system are worked out in detail separately. The equations of both concepts can be merged together to gain the total set of equations for the adjustable gravity equilibrator.

Double-cam transmission (DCT)

Figure 3 shows the parameters that were used to calculate the shape of the cams. Cam 1 is fixed on an axis A and attached to the mass of the system and cam 2 is fixed on an axis B and attached to the torsion bar(s). Both axes A and B are placed at the same height. The horizontal distance x between A and B can be chosen arbitrarily. The radius of the first cam $r_1(\alpha)$ and the radius of second cam $r_2(\beta)$ added together are always equal to x . Thus the point of contact C between the two cams is always situated somewhere on the horizontal line between A and B . Point C is also the point where the cable moves over from cam 1 to cam 2. The force F in the cable depends on the exerted moment on cam 1, M_{mass} , and the corresponding radius of cam 1. The same force in the cable also depends on the exerted moment on cam 2, M_{bars} ,

and the corresponding radius of cam 2. Thus for F it holds:

$$F = \frac{M_{mass}}{r_1} = \frac{M_{bars}}{r_2} \quad (4)$$

Since the length y of the cable is fixed, for small $d\alpha$ and $d\beta$ it holds:

$$dy = r_1(\alpha)d\alpha = r_2(\beta)d\beta \quad (5)$$

When we combine Eqn. (4) and Eqn. (5) we get:

$$M_{mass}d\alpha = M_{bars}d\beta \quad (6)$$

When we fill in M_{mass} from Eqn. (1) and M_{bars} from Eqn. (2), we can write:

$$\underbrace{mgL\sin\alpha}_{M_{mass}}d\alpha = \underbrace{k\beta}_{M_{bars}}d\beta \quad (7)$$

where k is the required stiffness of the torsion bar(s). This equation is only valid for small values of α and β . To get an equation which is valid for all values of α and β we can integrate Eqn. (7):

$$mgL \int \sin\alpha d\alpha = k \int \beta d\beta \quad (8)$$

The solution to Eqn. (8) is:

$$mgL(C_1 - \cos\alpha) = k\left(\frac{1}{2}\beta^2 + C_2\right) \quad (9)$$

where C_1 and C_2 are the integration constants of the indefinite integrals. Since the torsion bar(s) have no rotation at starting position, no moments acts on the pivot point when $\alpha = 0$ and $\beta = 0$. Thus when we substitute $\alpha = 0$ and $\beta = 0$ in Eqn. (9), this equation has to be equal to zero:

$$mgL(C_1 - 1) = kC_2 = 0 \quad (10)$$

Now it is clear that $C_1 = 1$ and $C_2 = 0$. Eqn. (9) can now be written as:

$$mgL(1 - \cos\alpha) = k\frac{1}{2}\beta^2 \quad (11)$$

This equation provides us an equation for β which depends on α , in such a way that Eqn. (3) holds. We are now able to calculate the angle of rotation of the torsion bars for every angle of rotation of the mass:

$$\beta(\alpha) = \sqrt{\frac{2mgL(1 - \cos\alpha)}{k}} \quad (12)$$

The required angle of rotation β of the torsion bar(s), can be influenced by the stiffness k of the torsion bar(s). If k is increased, the required angle of rotation β will decrease and vice versa. We decided to add a transmission parameter T to the equations, which makes it easy to determine a desired maximum value of β . To introduce this parameter T , we consider the case where $\alpha = \frac{\pi}{2}$. When we take into account Eqn. (3), we can write (and introduce T at the left hand side):

$$TmgL\sin\frac{\pi}{2} = -k\sqrt{\frac{2mgL(1 - \cos\frac{\pi}{2})}{k}} \quad (13)$$

Since T is introduced at the left hand side, the right hand side has to change as well. The variable at the right hand side which is still unknown, is the required stiffness k of the torsion bars. With Eqn. (13) an equation for this new k can be determined, which now depends on T :

$$k = \frac{1}{2}mgLT^2 \quad (14)$$

With Eqn. (12) and Eqn. (14) a new equation for β , with the extra constant T , can be defined:

$$\beta(\alpha) = \frac{2}{T}\sqrt{1 - \cos\alpha} \quad (15)$$

We are now able to choose a value for T in such a way that the required maximum value of β is equal to a desired value. The stiffness k is influenced by this value of T too, but in such a way that the system keeps statically balanced. Theoretically T has no limits. However, from Eqn. (19) and Eqn. (20) one can see that when $T \gg 1$ or $T \ll 1$, the difference in size of the cams will be large, which is not desirable for practical reasons. Large cams increase the total size of the system, whereas small cams require high tolerances.

Since β with respect to α is now known, the shapes of cam 1 and cam 2 can be determined. For the shapes of the cams it holds:

$$x = r_1(\alpha) + r_2(\beta) \quad (16)$$

$$r_1(\alpha) = x - r_2(\beta) \quad (17)$$

$$r_2(\beta) = x - r_1(\alpha) \quad (18)$$

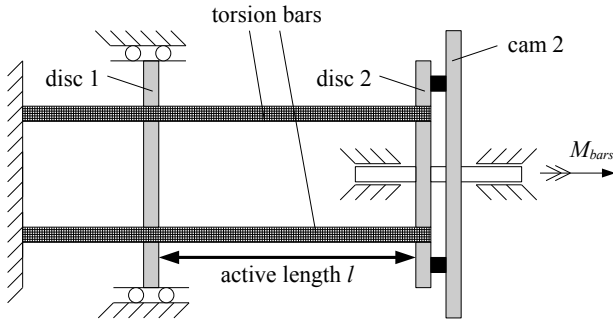


FIGURE 4. Schematic representation of two torsion bars (with solid square cross section) placed in parallel. Disc 2 (which can rotate) is connected to cam 2, and disc 1 (which can not rotate) can slide along the torsion bars to adjust the active length l .

When we now fill in Eqn. (4), for $r_1(\alpha)$ and $r_2(\beta)$ we can write respectively:

$$r_1(\alpha) = \frac{xM_{mass}}{M_{mass} + M_{bars}} = \frac{x\sin\alpha}{\sin\alpha + T\sqrt{1 - \cos\alpha}} \quad (19)$$

$$r_2(\alpha) = \frac{xM_{bars}}{M_{mass} + M_{bars}} = \frac{xT\sqrt{1 - \cos\alpha}}{\sin\alpha + T\sqrt{1 - \cos\alpha}} \quad (20)$$

By using a software package like MATLAB, the centroide (i.e. the contour of the shape) of each cam can be plotted on a graph. When the maximum angle of α or β is $< 2\pi$ rad, the centroide of the cam will not be a closed line. The centroide can be closed arbitrarily, as long as the functioning of the cams is not influenced.

Adjustable active length of torsion bar(s)

Figure 4 shows a schematic representation of two torsion bars with adjustable active length l . In general, n torsion bars are placed in parallel and fixed in disc 1 and disc 2. Disc 2 is connected to cam 2 and disc 1 can slide along the torsion bars. To easily clamp the torsion bars, a square cross section instead of a circular cross section is used. Because disc 1 is able to slide, the active length l can be changed and the system is adjustable on a continues range. Adjusting l is energy-free only if the torsion bars are not rotated, thus when $\beta + \beta_0 = 0$ rad. In other configurations, considerable effort may be required.

The required stiffness k of the gravity equilibrator, for a specific mass m , can be determined with Eqn. (14). For a statically balanced system, this stiffness k should be equal to the stiffness of the torsion bars. The relation in Eqn. (2) of the stiffness k_c of torsion bars with a circular cross section, does not hold anymore, since now torsion bars with a square cross section are used. The

stiffness k_s of torsion bars with a solid square cross section is [8]:

$$k_s = 0.1406G \frac{nw^4}{l} \quad (21)$$

where w is the width of one of the sides of the square cross section. By adjusting l , k_s is changed and thus a different mass can be statically balanced. When a specific material is used for the torsion bars (G is chosen), we still have to chose values for the parameters n and w . w is restricted by the maximum shear stress in the torsion bars. Therefore the following relation should be taken into account [8]:

$$w < \frac{1.482\tau_{max}l}{G\beta_{max}} \quad (22)$$

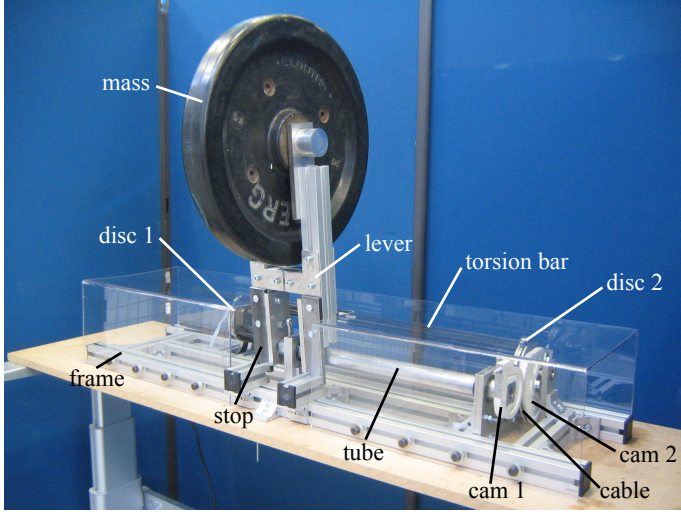
where τ_{max} is the maximum shear stress and β_{max} is the maximum angle of rotation of the torsion bar(s). With MATLAB, all possible combinations of n , w and l , taking into account Eqn. (22), can be listed.

We are able to influence the right hand side of Eqn. (22), by determining β_{max} . We can choose a specific value of β_{max} , by choosing a proper value of T in Eqn. (15). The amount of possible combinations of n , w and l thus is influenced by the value of T .

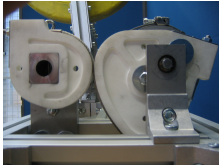
Once we have chosen n and w , the required active length l of the torsion bars for a specific mass m is known. When a range of $m_{min} \leq m \leq m_{max}$ is chosen, a range of $l_{min} \leq l \leq l_{max}$ can be determined. This range of l indicates the minimum and maximum required active length of the torsion bars, to reach a certain range of adjustability for m .

RESULTS

A prototype was built to verify the working principle of our design. A picture of the prototype can be seen in Fig. 5 and a schematic overview of the prototype can be seen in Fig. 6. With the aid of the schematic overview the prototype will be explained in more detail. Disc 1 is a circular disc with square cut-outs to hold the torsion bars (see Fig. 5(d)). Disc 1 can slide along the torsion bars to adjust the active length l . At the other side, the torsion bars are fixed in disc 2. Disc 2 is connected to cam 2 by a prismatic joint, which is made of two slide bearings which slide along two pins (see Fig. 5(c)). This prismatic joint makes it able that disc 2 has the same angle of rotation as cam 2, however the distance between disc 2 and cam 2 can vary. This margin is needed since the torsion bars are rotated on the longitudinal axis of disc 1 and disc 2, and not on their own longitudinal axis. As a result, the torsion bars are also bended when they are rotated and disc 1 and disc 2 are moved towards one another. Since disc 2 is able to move, cam 2 can be fixed on the axis and connected



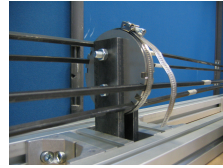
(a)



(b)



(c)



(d)

FIGURE 5. Pictures of the prototype: (a) a general overview, (b) the two cams in starting position, (c) the connection between cam 2 and disc 2 and (d) disc 1

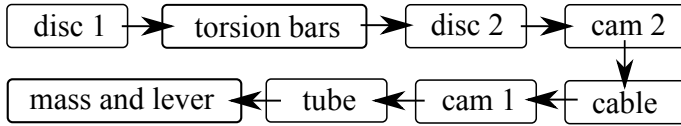


FIGURE 6. Schematic overview of the prototype. One starts with sliding disc 1 at the right position, which finally results in a statically balanced system for the mass and lever.

to cam 1 by a cable (see Fig. 5(b)). Cam 1 is connected to the lever and mass by a tube. Due to two mechanical stops, the mass can only be rotated between $0 \leq \alpha \leq \frac{\pi}{2}$ rad. The width and depth of the frame of the prototype are 1173 mm and 280 mm respectively.

Dimensional design

With MATLAB we calculated the centroids of the cams and all possible combinations of n , w and l according to the design requirements. The design parameters used for the calculations are shown in Tab. 2. Most of the parameters follow from the design requirements and material properties of the torsion bars. However, x and T could be chosen arbitrarily. We chose x as

TABLE 2. Design parameters of the prototype, used to calculate the centroids of the cams and all possible combinations of n , w and l

Parameter	Symbol	Value
Angle of rotation of mass	α	$0 < \alpha < \frac{\pi}{2}$ rad
Mass	m	$20 < m < 30$ kg
Gravity constant	g	9.81 m/s ²
Length of lever	L	400 mm
Distance between A and B	x	130 mm
Transmission parameter	T	2
Shear modulus	G	78 GPa
Maximum shear stress	τ_{max}	680 MPa
Active length of torsion bar(s)	l	$l < 1000$ mm

TABLE 3. Four possible combinations of n , w , l_{min} and l_{max} for the prototype. Every row provides a possible combination, which is just as good as the other ones. One can pick one solution using criteria like smallest length, smallest difference between l_{min} and l_{max} , smallest width, etc.

l_{max} [mm]	l_{min} [mm]	w [mm]	n
724	483	6	8
815	543	6	9
839	559	7	5
906	604	6	10

small as possible, in such a way that the size of the cams did meet the minimum required bending radius of the cable. $T = 2$ was chosen to decrease β_{max} , which results in an enlargement of the amount of possible combinations of n , w and l .

MATLAB provided all suitable combinations of n , w and l . For practical reasons we excluded all solutions where $n > 10$, since we did not want to use many torsion bars for the first prototype. The four possible combinations of n , w and l left, can be seen in Tab. 3. For building the prototype we picked the solution which provided the smallest total length, which is the first one of Tab 3.

Experimental results

Figure 7 shows the force-deflection diagram of the cable between the cams. The cable was placed in a universal testing ma-

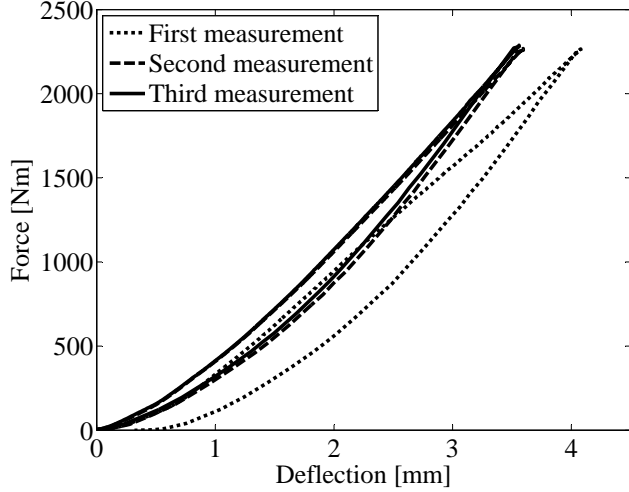


FIGURE 7. Three consecutive measurements with the stainless steel cable between the cams. During each measurement, the cable was stretched with a maximum force of 2280 N and released again.

chine M250-2.5 CT of Testometric and three consecutive measurements were done. The force-deflection diagram shows that the strain of the cable is relatively big at the beginning of the measurements. The consequence is that the operation of the DCT is influenced at the beginning of the rotation. Since the cable is relatively elastic in this domain, cam 2 rotates less than expected. However, when we pre-tension the cable, the cable already is stretched at the beginning. In this situation we do not have to deal with the relatively big strain and the operation of the DCT is not influenced by this phenomenon anymore.

In our prototype it was not possible to tighten the cable, since this would change the initial angle of both cams. However, since the two mechanical stops make sure that the mass can only rotate between $0 \leq \alpha \leq \frac{\pi}{2}$ rad, we are able to pre-tension the torsion bars, without influencing the starting position of the cams. In that situation $\beta_0 \neq 0$ rad and at the beginning of the rotation a moment of $M_0 = k\beta_0$ is exerted on cam 2. Because of M_0 , the cable is pre-tensioned. After this the cams can be placed in their initial position.

Since now $\beta_0 \neq 0$, Eqn. (3) does not hold anymore. When $\alpha = 0$ rad, $M_{mass}(0) = 0$. However, when $\beta = 0$ rad, $M_{bars}(0) = M_0$. In this situation the mass will not be perfectly statically balanced. To be still able to verify the operation of our DCT, we removed the mass and lever from the prototype and measured the exerted moment on cam 1 with the universal testing machine. A tube is fixed in between cam 1 and a testing disc. Around the testing disc a cable is placed. This cable is moved up and down by the universal testing machine and since the radius of the testing disc is known and the force in the cable is measured, the exerted moment on cam 1 can be calculated. The values of these measurements will not start at zero, but at M_0 . Three con-

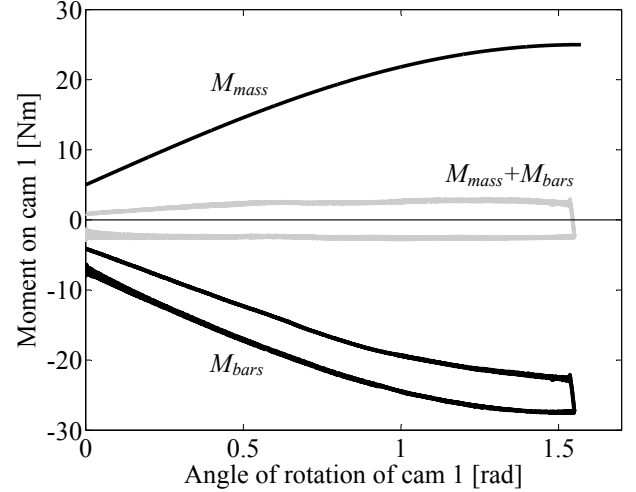


FIGURE 8. Three consecutive measurements on cam 1 of M_{bars} , with $n = 2$ and $l = 710$ mm. M_{mass} is the calculated theoretical value.

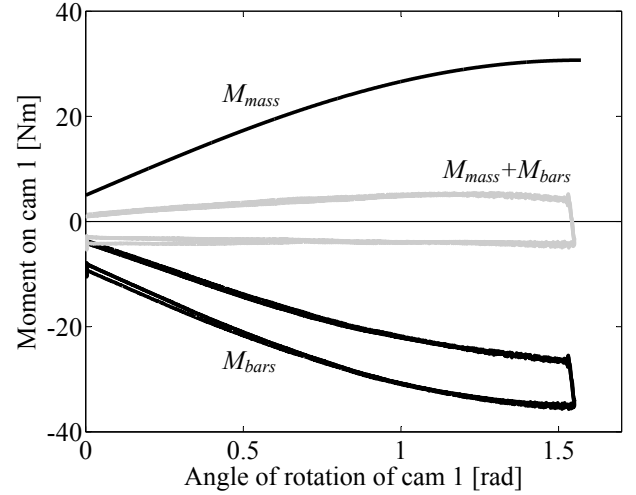


FIGURE 9. Three consecutive measurements on cam 1 of M_{bars} , with $n = 2$ and $l = 554$ mm. M_{mass} is the calculated theoretical value.

secutive measurements were done (see Fig. 8), with $n = 2$ and $l = 710$ mm. According to Eqn. (3), the measured value of M_{bars} summed up with the theoretical value of M_{mass} , should be equal to zero. M_{mass} can be calculated with Eqn. (14) and Eqn. (21):

$$M_{mass} = \frac{0.1406Gnw^4}{\underbrace{\frac{1}{2}lT^2}_{mgL}} \sin \alpha + M_0 \quad (23)$$

Figure 8 shows that the values of $M_{mass} + M_{bars}$ indeed are located around the x-axis.

When M_{mass} of the system changes (m changes), M_{bars} should change (adapt l) to make sure that Eqn. (3) still holds. We did three consecutive measurements (see Fig. 9), with $n = 2$ and $l = 554$ mm. This figure shows that the values of $M_{mass} + M_{bars}$ are located around the x-axis.

DISCUSSION

The measurements show that the DCT generates a perfectly statically balanced system which is adjustable for different masses by changing l . However, the measurements were carried out while $\beta_0 \neq 0$. The system should also work for $\beta_0 = 0$ rad. Otherwise it is not possible to adapt l in an energy-free manner, since for $\beta_0 \neq 0$ rad the torsion bars will always be rotated, even at the beginning. In the existing prototype it was not possible to pre-tension the cable without changing β_0 . For future developments, several other ways to pre-tension the cable without changing β_0 are possible.

A solution could be to use two cables between the cams instead of one, where both cables are placed in opposite direction. It is now possible to pre-tension both cables to the same extent, through which the starting angle of the cams does not change. Another option could be to make a mechanical stop on both cams, through which they can only be rotated into one direction. Then the cable can be pre-tensioned without affecting the starting angle of rotation of the cams.

It is also possible to look for solutions where no cable is used at all. Other possibilities for connecting both cams are using a band or teeth profiles. A band has the advantage that its thickness is small in comparison to the diameter of a cable. This means that the error of the two radii of the cams will be smaller. The total stress in the band is [21]:

$$\sigma_b = \frac{F_b}{tb} + \frac{Et}{D} \quad (24)$$

where F_b is the force in the band, t is the band thickness, b is the band width, E is the modulus of elasticity and D is the minimum required diameter of the cams. Assumed is that no normal forces are present in the band. With MATLAB all possible combinations of t , b and D can be determined. In our prototype a band with a thickness of 0.2 mm and a width of 30 mm could have been used instead of the cable. Since the cable exists of many thin elements, its area moment of inertia is smaller than that of the band. This implies that for the band stiffness due to bending is higher than for the cable, which may influence the results. This extra stiffness should be compensated, thus the required stiffness of the torsion bar(s) should be different when a band instead of a cable is used.

When the cams are designed with teeth profiles, no connection elements are needed at all. However, obtaining the correct teeth profiles requires difficult mathematical calculations on

which research is still going on [13]. High friction forces are present between the teeth too [12]. To actually build the cams with teeth profiles is still an issue as well.

The measurements showed that a certain amount of hysteresis is present in the system. It is assumed that the hysteresis is mainly caused by the friction of the slide bearings used in the prototype. When we look at Fig. 8 we see that 4.5 Nm hysteresis is present in the system, when $\alpha = \frac{\pi}{2}$ rad. Only the static friction coefficient of the slide bearings is known, which is 0.11. The dynamic friction coefficient will probably be lower. However, since the system was measured with a very low speed of 200 mm/min, we use the static friction coefficient to make an estimation.

Slide bearings were used on the tube between cam 1 and the mass, and on the pins of the prismatic joint. Figure 10 shows a schematic overview of cam 1 and cam 2. The free body diagram is split up in point C, to show the force F present in the cable. The force equilibrium of cam 1 provides us the total force $F_A = 618$ N on pivot point A of cam 1, which in the prototype is the tube. The force equilibrium of cam 2 provides us the total force on the pins, which is $2F_j = 2084$ N. For the tube a maximum (static) friction force of $618 \cdot 0.11 = 68$ N is calculated and for the pins a maximum (static) friction force of $2084 \cdot 0.11 = 229$ N is calculated. To compare these values with the value of the hysteresis, we have to determine the moments to counteract the friction instead of the forces. The radius of the tube is 0.0175 m, thus the extra moment needed to counteract the friction for the tube is $68 \cdot 0.0175 = 1.2$ Nm.

The friction force of the pins is perpendicular to disc 2. Since the torsion bars bend out of plane during rotation, the force in the torsion bars can be resolved into a radial, a tangential and a perpendicular force to disc 2. If this perpendicular force is bigger than the friction force of the pins, disc 2 starts to slide on the bearings. The tangential force in the torsion bars, creates an extra moment on point B. The relation between the tangential and perpendicular force in the torsion bars, is approximately the same as the relation between the vertical distance and horizontal distance between both ends of the rotated torsion bars. Since the vertical distance is 710 mm and the horizontal distance is 50 mm, the tangential force is 16 N. The radius of disc 2 is 50 mm, thus the extra moment needed to counteract the friction is $16 \cdot 0.05 = 0.8$ Nm.

To conclude, $1.2 + 0.8 = 2.0$ Nm is (static) friction caused by the slide bearings when $\alpha = \frac{\pi}{2}$ rad. This holds for the upper and lower line of M_{bars} in Fig. 8. The other 0.5 Nm of the hysteresis is probably caused by the radial ball bearings, the cable, deformation of parts and the cams, and measurement errors. A certain amount of friction in the system is advisable, since in this way small errors in the system can be set off.

In the calculations of the centroids of the cams it is assumed that the connection of the tube between the mass and cam 1 is rigid. Actually the stiffness of the tube should be taken into account, since it affects the angle of rotation of cam 1. The maxi-

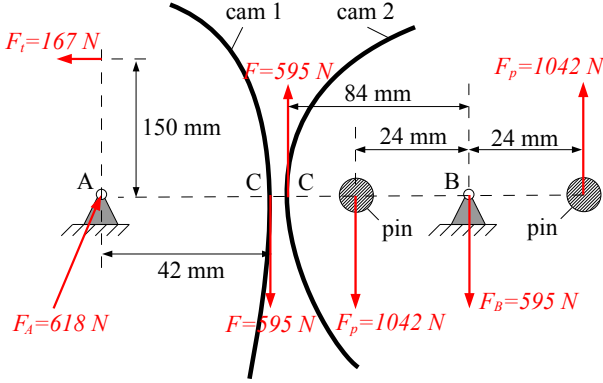


FIGURE 10. Force equilibrium on point A and point B for $\alpha = \frac{\pi}{2}$ rad (cams are split up in point C). The force F_t of the universal testing machine is 167 N. With the moment equilibrium around point A the force F in the cable can be calculated: $F = 595$. The total force F_A on point A is thus $\sqrt{595^2 + 167^2} = 618$ N. Since now F is known, the force F_p on each pin can be calculated with the moment equilibrium around point B.

moment exerted by the mass is:

$$M_{mass}\left(\frac{\pi}{2}\right) = 25 \cdot 9.81 \cdot 0.4 \cdot \sin\left(\frac{\pi}{2}\right) = 98.1 \text{ Nm}$$

The stiffness of the tube is equal to $k_{tube} = 11 \cdot 10^3$ Nm/rad. The angle of rotation of the tube, due to M_{mass} , is:

$$\alpha^* = \frac{98.1}{11 \cdot 10^3} = 0.0089 \text{ rad}$$

Since this error is $< 1\%$, we think the assumption of the tube to be rigid is acceptably.

For the prototype it holds that $0 \leq \alpha \leq \frac{\pi}{2}$ rad, $L = 400$ mm and $l < 1000$ mm. The range of $20 \leq m \leq 30$ kg was not reached, since the system only worked for $\beta_0 = 0.5$ rad. When $\beta_0 = 0.5$ rad, the total angle of rotation β_{max} of the torsion bars is increased with 0.5 rad. From Eqn. (22) one can then see that l should be larger too, in case that w is still smaller than the right hand side of the equation. When l increases, the stiffness of the torsion bars decreases. With $\beta_0 = 0.5$ rad, l_{min} is about 700 mm, which gives $m_{max} = 21$ kg.

With the calculations of the centroids of the cams, the exerted moments M_{mass} and M_{bars} can be chosen arbitrarily. Thus the calculations can be performed for other cases as well. In general M_{mass} is the required output of the system and M_{bars} is the moment exerted by a mechanism which supplies energy. An example of another case for the new adjustable gravity equilibrator is a hospital bed. The legs of the bed are crossed and the care taker is able to adjust the height of the bed by changing the angle

of the legs. When the torsion bars and cams are placed in the pivot point of the legs, the care taker can adjust the height with hardly any operation effort. The stiffness of the torsion bars can be adjusted to the weight of the patient.

CONCLUSION

- A theoretical perfectly balanced system using torsion bars is achieved by a new DCT design.
- A general method to calculate the shape of the two cams of the DCT is presented, which makes it possible to apply the method to other applications as well.
- Scaling of the DCT is possible and the range of the angles of rotation of both cams can be chosen.
- The gravity equilibrator is adjustable for a self-selected continuous range of masses, by changing the active length of the torsion bars.
- One is able to restrict the number and size of the torsion bars if wanted.
- Adjustment of the active length is energy-free when the torsion bars have no rotation.
- A prototype was built and it was shown that the system is statically balanced for different active lengths of the torsion bars.
- Technical improvements on the prototype are still possible.

ACKNOWLEDGMENT

We want to thank the InteSpring team, Koen Davina and Guido Oud for their support and assistance in realizing the prototype and this paper.

NOMENCLATURE

b	band width [m]
d	diameter of torsion bar with circular cross section [m]
D	minimum required diameter of cams [m]
E	modulus of elasticity [Pa]
F	cable force [N]
F_b	band force [N]
F_p	force on prismatic joint [N]
F_t	force of tensile testing machine [N]
F_A	force on point A
F_B	force on point B
g	gravity constant [m/s^2]
G	shear modulus [Pa]
k	required stiffness of torsion bar(s) [Nm/rad]
k_c	stiffness of torsion bar(s) with circular cross section [Nm/rad]
k_s	stiffness of torsion bar(s) with square cross section [Nm/rad]
k_{tube}	stiffness of tube [Nm/rad]
l	active length of torsion bar(s) [m]
l_{min}	minimum active length of torsion bar(s) [m]

l_{max}	maximum active length of torsion bar(s) [m]
L	length of lever [m]
m	mass [kg]
m_{min}	minimum mass [kg]
m_{max}	maximum mass [kg]
M_1	exerted moment on cam 1 [Nm]
M_2	exerted moment on cam 2 [Nm]
M_{bars}	exerted moment by torsion bar(s) [Nm]
M_{mass}	exerted moment by mass [Nm]
n	number of torsion bars [-]
r_1	radius of cam 1 [m]
r_2	radius of cam 2 [m]
t	band thickness [m]
T	transmission parameter [-]
w	width of torsion bar(s) with square cross section [m]
x	horizontal distance between axis of cam 1 and cam 2 [m]
y	cable length [m]
α	angle of rotation of torsion bar(s) [rad]
α^*	angle of rotation of tube relative to α [rad]
β	angle of rotation of mass [rad]
β_0	initial angle of rotation of torsion bar(s) [rad]
β_{max}	maximum angle of rotation of torsion bar(s) [rad]
σ_b	total stress in band [Pa]
τ_{max}	maximum shear stress [Pa]

REFERENCES

- [1] van Dorsser, W., Barents, R., Wisse, B., Schenk, M., and Herder, J., 2008. "Energy-free adjustment of gravity equilibrators by adjusting the spring stiffness". *Journal of Mechanical Engineering Science*, **222**, April, pp. 1839–1846.
- [2] Kobayashi, K., 2001. "Comparison between spring balancer and gravity balancer in inertia force and performance". *Journal of Mechanical Design*, **123**, December, pp. 549–555.
- [3] Herder, J., 2001. "Energy-free systems". PhD Thesis, Delft University of Technology, Delft, November.
- [4] van Osch, F., 2010. Mechanical spring design guide based on absorbed potential energy. June.
- [5] Holland container innovations. URL <http://www.hcinnovations.nl>.
- [6] Claus, M., 2008. "Gravity balancing using configurations of torsion bars". MS Thesis, Delft University of Technology, Delft, December.
- [7] Dynteq flatscreenlift. URL <http://www.dynteq.nl>.
- [8] Chironis, N. P., 1961. *Spring Design and Application*. McGraw-Hill Book Company, Inc., New York.
- [9] Geary, P., 1960. *Torsion Devices*. British Scientific Instrument Research Association, South Hill, Chislehurst, Kent.
- [10] Litvin, F., Fuentes-Aznar, A., Gonzalez-Perez, I., and Hayasaka, K., 2009. *Noncircular Gears, design and generation*. Cambridge University Press, New York.
- [11] Mundo, D., 2005. "Geometric design of a planetary gear train with non-circular gears". *Mechanism and Machine Theory*, **41**, August, pp. 456–472.
- [12] Danieli, G., and Mundo, D., 2004. "New developments in variable radius gears using constant pressure angle teeth". *Mechanism and Machine Theory*, **40**, August, pp. 203–217.
- [13] Tsay, M., and Fong, Z., 2003. "Study on the generalized mathematical model of noncircular gears". *Mathematical and Computer Modelling*, **41**, August, pp. 555–569.
- [14] Ferguson, R., Daws, L., and Kerr, J., 1975. "The design of a stepless transmission using non-circular gears". *Mechanism and Machine Theory*, **10**, January, pp. 467–478.
- [15] Kazerounian, K., and Furu-Szekely, Z., 2005. "Parallel disk continuously variable transmission (pdcvt)". *Mechanism and Machine Theory*, **41**, September, pp. 537–566.
- [16] Parsons, F., 1987. Continuously variable transmission, March. US Patent Number 4,650,442.
- [17] van Blaricom, T., 1994. Continuously variable transmission, June. US Patent Number 5,324,239.
- [18] Nuvinci. URL <http://www.fallbrooktech.com>.
- [19] Clellan, W. M., 2008. Non-helical torsion spring system, July. Patent Application Publication Number US 2008/0179799 A1.
- [20] Drexhage, G., 1986. Adjustable torsion bar assembly, July. US Patent Number 4,597,568.
- [21] Kuntz, J., 1995. "Rolling link mechanisms". PhD Thesis, Delft University of Technology, Delft, May.

Appendix A

Material properties of high-class spring steel

To calculate the active length l , the width w and the number n of torsion bars required for the prototype, the values of the shear modulus G and the maximum shear stress τ_{max} of high-class spring steel are needed. A torsion test and tensile test were carried out to define the shear modulus G and the shear strength τ_y respectively. In the calculations the shear strength is taken as the maximum shear stress. The tests were performed with a torsion bar of high-class spring steel with $l = 0.5$ m and a solid round circular cross section with a diameter of $d = 3$ mm.

With the torsion test the stiffness of the torsion bar was measured as $k_c = 1.235$ Nm/rad (see Fig. A.1(a)). With the formula for the stiffness of a torsion bar with a solid circular cross section the shear modulus can now be calculated, since all other variables of this formula are known [8]:

$$k_c = \frac{\pi d^4 G}{32l} \quad (\text{A.1})$$

Thus the shear modulus is:

$$G = \frac{32k_c l}{\pi d^4} = \frac{32 \cdot 1.235 \cdot 0.5}{\pi \cdot 0.003^4} = 78 \text{ GPa}$$

With the tensile test the yield strength σ_y could be estimated from the stress-strain curve (see Figure A.1(b)). The value of the yield strength was selected as 1.4 GPa. For the shear strength it holds:

$$\tau_y \approx 0.6\sigma_y \quad (\text{A.2})$$

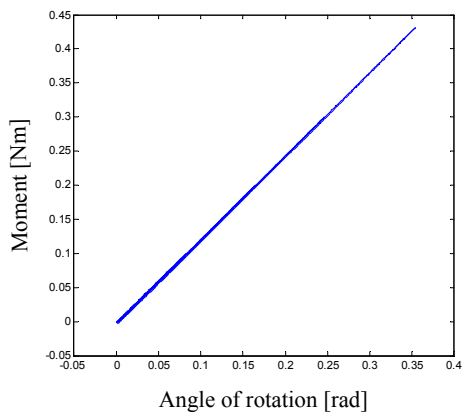
For the calculations the shear strength is taken as:

$$\tau_y \approx 0.6\sigma_y \approx 0.6 \cdot 1.4 \cdot 10^9 \approx 850 \text{ MPa}$$

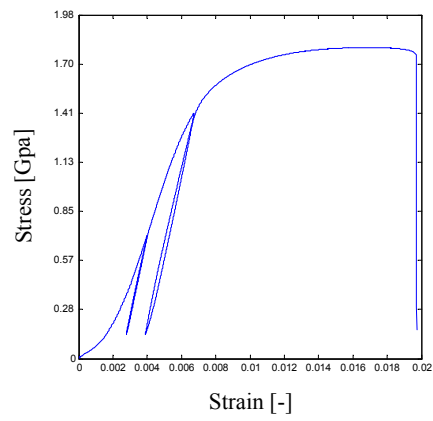
For the prototype a safety factor was introduced, therefore we actually used:

$$\tau_y = 0.8 \cdot 850 = 680 \text{ MPa}$$

The grippers of the tensile testing machine are based on friction. Since high-class spring steel is hardened steel, it is difficult to fasten the ends of the torsion bar. The peaks in the graph are likely to be the cause of slip in the grippers during the measurement.



(a)



(b)

Figure A.1: Measurement data of a torsion bar with a solid circular cross section with $l = 0.5$ m and $d = 3$ mm: (a) torsion test and (b) tensile test

Appendix B

Stiffness properties of torsion bars

B.1 Compound torsion bars

Compound torsion bars have a common axis of rotation, which can be seen in Fig. B.1. In this configuration a torsion bar is not only subjected to pure torsion when it is rotated, since there is an offset between the common axis of rotation and the torsion bar itself. This means that the stiffness properties of the compound torsion bars are influenced by this offset. The relation between the offset and the exerted moment by a torsion bar can be determined with the software package ANSYS. The variables used for the simulation are shown in Tab. B.1.

The exerted moment of a torsion bar was simulated for different values of the offset (see Fig. B.2). For the exerted moment of a torsion bar with a solid circular cross section it holds [8]:

$$M = k_c \beta = \frac{\pi d^4 G}{32l} \beta \quad (\text{B.1})$$

where k_c is the the stiffness of one torsion bar, β is the angle of rotation, d is the diameter of the circular cross section, l is the (active) length and G is the shear modulus of the material. When one fills in Eqn. (B.1) with the values used in the simulation and $G = 78$ GPa, one gets:

$$M = \frac{\pi \cdot 0.006^4 \cdot 78e9 \pi}{32 \cdot 0.483} \frac{\pi}{2} = 32.3 \text{ Nm}$$

From the graph of Fig. B.2 it is seen that the exerted moment of the torsion bars increases rapidly when the offset is bigger than 0.05 m.

Table B.1: ANSYS model variables

Material properties	
Poisson's ratio ν	0.3
Density ρ	7850 $\frac{\text{kg}}{\text{m}^3}$
Modulus of elasticity E	210 GPa
Torsion bars	
Number n	6
Active length l	483 mm
Diameter d	6 mm
Angle of rotation β	$\frac{\pi}{2}$ rad

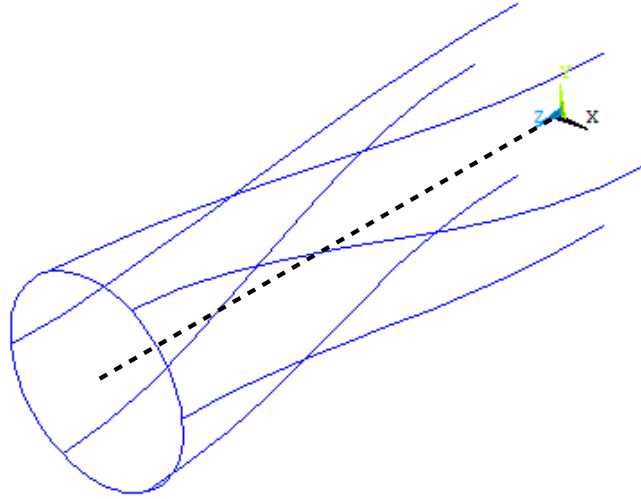


Figure B.1: Rotated compound torsion bars (solid lines) with common axis of rotation (dashed line)

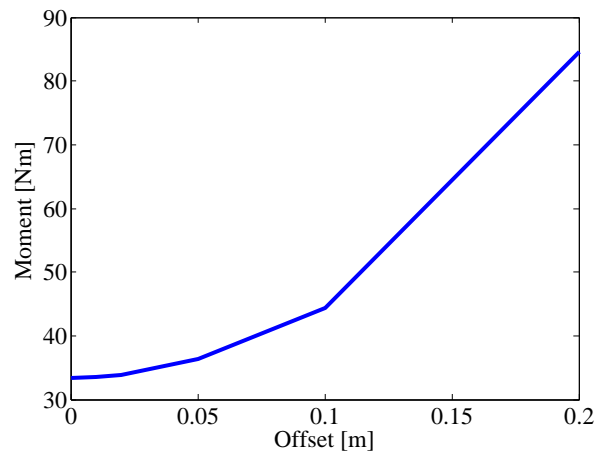


Figure B.2: Relation between offset and exerted moment for compound torsion bars

B.2 Axial forces

The change in stiffness k_P of a torsion bar with a solid circular cross section subjected to an axial force P is equal to [9]:

$$k_P = \frac{d^2 P}{8l} \quad (\text{B.2})$$

where P is taken positive when a tensile force is applied and P is taken negative when a compressive force is applied. When a compressive force is applied, one should also take into account buckling theory. The total stiffness k_{tot} of a torsion bar with a solid circular cross section subjected to twist and an axial force can now be defined as:

$$k_{tot} = \frac{\pi d^4 G + 4d^2 P}{32l} \quad (\text{B.3})$$

The nominal stress σ_n due to an axial force in a torsion bar with a solid circular cross section is defined as [9]:

$$\sigma_n = \frac{4P}{\pi d^2} \quad (\text{B.4})$$

According to Eqn. B.4 for P one can now write:

$$P < \frac{\pi d^2 \sigma_{max}}{4} \quad (\text{B.5})$$

where σ_{max} is the maximum nominal stress in the torsion bar. For Eqn. B.5 one can also write:

$$4Pd^2 < \pi d^4 \sigma_{max} \quad (\text{B.6})$$

The maximum total stiffness of a the torsion bar with a solid circular cross section subjected to twist and an axial force can now be defined as:

$$k_{max} = \frac{\pi d^4 G + \pi d^4 \sigma_{max}}{32l} \quad (\text{B.7})$$

When taking $G = 78 \cdot 10^9$ and $\sigma_{max} = 1.4 \cdot 10^9$, it is clear to see that $\pi d^4 G \gg \pi d^4 \sigma_{max}$. Thus the stiffness of a torsion bar due to twist is hardly influenced by axial forces.

Appendix C

Proof of concept

A proof of concept was built to show the working principle of the system (see Fig. C.1). The two cams were made by a rapid prototyping technique. The centroids of the cams were calculated with $T = 1$ and $x = 100$ mm. Two torsion bars with a circular round cross section with $d = 3$ mm and $l = 705$ mm were used. The stiffness of the system could be halved by removing one of the torsion bars. The system should be able to balance a mass of 1.0 kg (one torsion bar) and 2.0 kg (two torsion bars) respectively, with $L = 180$ mm. In practice the system was able to balance a mass of 1.1 kg and 2.2 kg. Some small errors were introduced since the mass was placed at one side of the lever and not in the middle. During rotation the mass swung a little and the lever was not perfectly vertical in its initial position. Also the stiffness of the model will always be higher than the expected stiffness, since one always have to deal with friction in the system.

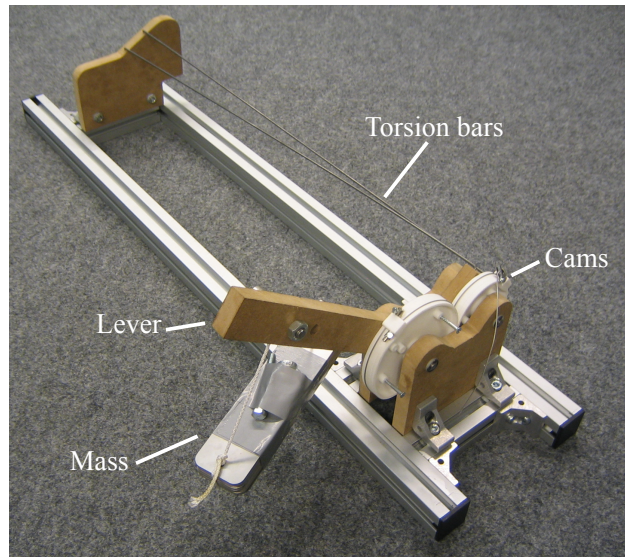


Figure C.1: Proof of concept

Appendix D

Prototype

D.1 Calculations

D.1.1 Cable

The stainless steel cable is equipped with screw thread at both ends, which makes it possible to tighten the cable around the cams with nuts. Screw thread can not be placed at every type of cable, a selection had to be made from cables with a 7 x 19 construction (see Fig. D.1). For the cables a minimum diameter d_{min} of the cams is required, which is defined as 25 times the diameter d_{cable} of the cable. When the minimum required diameter of the cams is known, the maximum force F_{max} in the cable can be calculated with:

$$F_{max} = \frac{m_{max}gL}{d_{min}/2} \quad (\text{D.1})$$

This maximum force may not exceed the breaking load F_{break} of the cable. Experience has shown that the maximum force in the cable should be at least as twice as small as the breaking load. From Tab. D.1 one can see that than a cable with a diameter of 3.5 mm is the smallest cable which is suitable for the prototype. Since the cams are not perfectly round and the force in the cable varies during the entire range of motion, the next cable in row, which has a diameter of 4 mm, is chosen for the prototype.

When the diameter of the cable is 4 mm, the minimum required diameter of the cams is 100 mm. The size of the cams depends on the distance x between the two centres of the cams, which can be calculated with the software package MATLAB. From Tab. D.2 it can be seen that the distance between the centres of both cams should be between 150 and 160 mm. However, since a cable with a higher breaking load than required was selected, the minimum required radius can be a little smaller, because the forces in the cable are relatively small. Suppose the maximum forces in the cable are as thrice as small as the breaking load, than the maximum forces in the cable still can be $\frac{8.34}{3} = 2.8$ kN. From Tab. D.2 one can see that when $x = 130$ mm, the maximum forces in the cable are 2.8 kN. To conclude, if $x = 130$ mm, the maximum forces in the cable are still three times smaller than the breaking load. To reduce the dimensions of the prototype, $x = 130$ mm was chosen instead of a value between 150 and 160 mm.

Table D.1: Cable properties

d_{cable} [mm]	d_{min} [mm]	F_{break} [kN]	F_{max} [kN]
1.5	38	1.25	6.3
2.0	50	2.08	4.7
2.5	63	3.26	3.8
3.0	75	4.69	3.1
3.5	88	6.39	2.7
4.0	100	8.34	2.4
5.0	125	13.00	1.9

Table D.2: Cam properties

x [mm]	d_{min} [mm]	F_{max} [kN]
100	64	3.7
110	70	3.4
120	78	3.0
130	84	2.8
140	90	2.6
150	98	2.4
160	104	2.3

Construction 7 x 19					
ø in mm	minimum breaking load		weight in kg/100 m	Ref. No.	
	kN	kg			
1,5	1,25	128	0,90	0160.10.15	
2,0	2,08	212	1,49	0160.10.20	
2,5	3,26	332	2,33	0160.10.25	
3,0	4,69	478	3,35	0160.10.30	
3,5	6,39	652	4,56	0160.10.35	
4,0	8,34	850	5,95	0160.10.40	
5,0	13,00	1330	9,30	0160.10.50	
6,0	18,80	1920	13,40	0160.10.60	
7,0	25,50	2600	18,20	0160.10.70	
8,0	33,40	3410	23,80	0160.10.80	
10,0	52,10	5310	37,20	0160.11.00	
12,0	75,10	7660	53,60	0160.11.20	
14,0	102,00	10100	72,90	0160.11.40	
16,0	133,00	13600	95,50	0160.11.60	

Figure D.1: Available stainless steel cables with construction 7 x 19

D.1.2 Transmission parameter T

For the prototype $T = 2$ was chosen, since then $\beta = 1$ radial. In this way it was possible to place the eight torsion bars symmetrically around the point of rotation, while some space was left to place a support in between (see Fig. D.2). The radius of the disc is chosen 0.05 m.

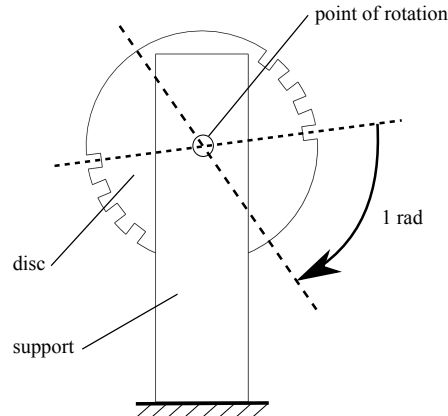


Figure D.2: Disc with square cut-outs for the torsion bars and the support which is fixed to the frame. When the disc is rotated 1 rad, the torsion bars just do not touch the support.

D.1.3 Shortening of compound torsion bars

When the compound torsion bars are rotated, they are subjected to twist and an axial displacement. This axial displacement is caused by the fact that the torsion bars are not rotated about their longitudinal axis, but around a common axis. Therefore the connection between the torsion bars and the cam in the prototype is not rigid and the torsion bars can move freely in axial direction. When no axial displacement is allowed, the torsion bars will be stretched and extra stress will appear in the torsion bars and the frame of the prototype. In the prototype the torsion bars are able to slide along two pins in slide bearings. The required length of the pins can be determined with a simple sketch of the configuration of the compound torsion bars (see Fig. D.3). The difference between the new length l^* and the nominal length l of the torsion bar is the required length of the pins. When we make two right triangles, $\triangle rrs$ and $\triangle sll^*$, l^* can be calculated with:

$$l^* = \sqrt{l^2 + 2r^2} \quad (\text{D.2})$$

The axial displacement of the torsion bars is biggest for the smallest length, which is $l = 483$ mm in our prototype. We have $r = 50$ mm, so l^* is equal to:

$$l^* = \sqrt{483^2 + 2 \cdot 50^2} = 488 \text{ mm}$$

The compound torsion bars shorten 5 mm when they are rotated $\frac{\pi}{2}$ radians. However, in our prototype they will just rotate 1 radial and shortening will be smaller. Though, to make sure, the free length of the pins is chosen twice the required length, which is $5 \cdot 2 = 10$ mm.

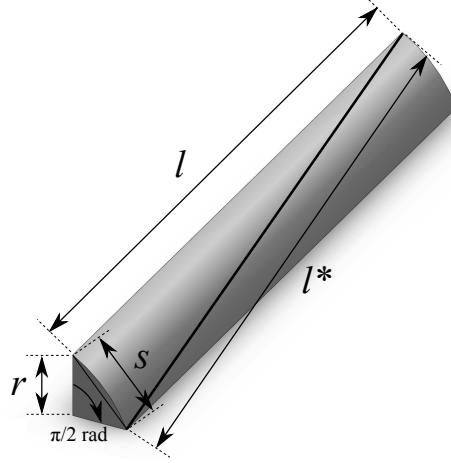


Figure D.3: Torsion bar (thick line) with nominal length l which is rotated $\frac{\pi}{2}$ rad. Since there is a distance r to the point of rotation, the length of the torsion bar will change to l^* after rotation.

D.1.4 Stiffness of rotating axes

The stiffness k_{tube} of a tube with a circular cross section is equal to [8]:

$$k_{tube} = \frac{\pi(d_{out}^4 - d_{in}^4)G}{32l} \quad (D.3)$$

where d_{out} is the outer diameter of the tube and d_{in} is the inner diameter of the tube. In the prototype the mass and cam 1 are connected by a tube. For this tube $d_{out} = 0.035$ m, $d_{in} = 0.031$ m and $l = 0.46$ m. Thus the stiffness of this tube is equal to:

$$k_t = \frac{\pi(0.035^4 - 0.031^4)80 \cdot 10^9}{32 \cdot 0.43} = 11 \cdot 10^3 \text{ Nm/rad}$$

For the tube between the cam and the measurement setup it holds:

$$k_t = \frac{\pi(0.018^4 - 0.015^4)80 \cdot 10^9}{32 \cdot 0.16} = 2.7 \cdot 10^3 \text{ Nm/rad}$$

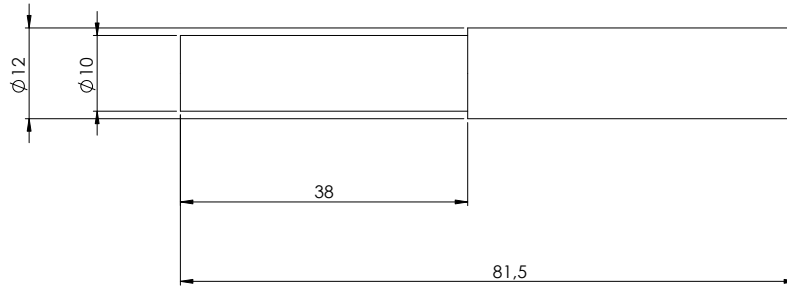
In Tab. D.3 the results for both tubes are shown.

Table D.3: Stiffness of rotating axes

Axis	Stiffness [Nm/rad]
Tube between mass and cam 1	$11 \cdot 10^3$
Tube between cam 1 and measurement setup	$2.7 \cdot 10^3$

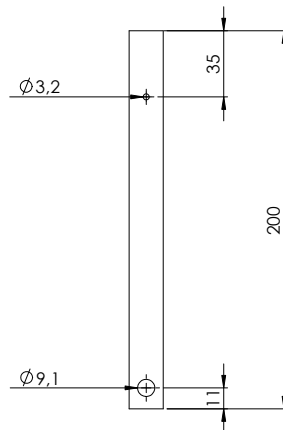
D.2 Drawings

D.2.1 General parts



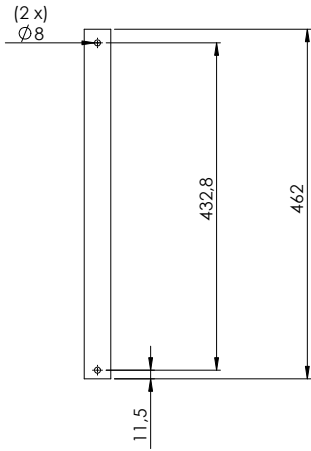
SolidWorks Student License
Academic Use Only

Indien niet anders aangegeven: Toleranties: Afstanden: 0,1 mm Hoeken: 0,5 gr	Aantal: 1	Materiaal: Staal
	Projectcode: V06.03	Afwerking: <afwerking>
InteSpring B.V. Rotterdamseweg 145 2628 AL Delft T +31 (0)15-2577008 F +31 (0)15-2788842	intespring	Naam: As 12x10 - kopie
Getekend door: Freeke van Osch	Datum: 19-10-2010	Schaal: 2:1 A4 Sheet 1 van 1



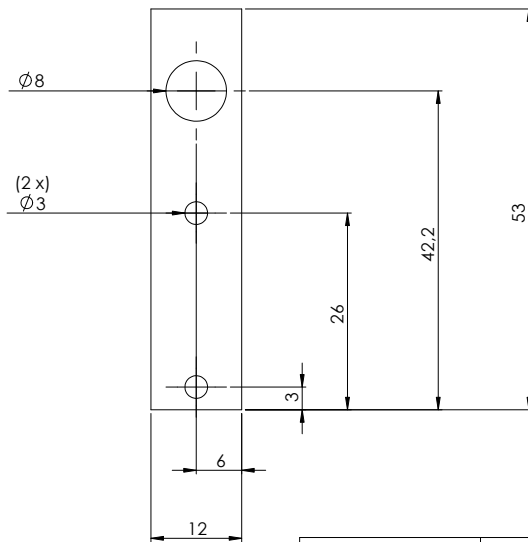
SolidWorks Student License
Academic Use Only

Indien niet anders aangegeven: Toleranties: Afstanden: 0,1 mm Hoeken: 0,5 gr	Aantal: 1	Materiaal: Staal
	Projectcode: V06.03	Afwerking: <afwerking>
InteSpring B.V. Rotterdamseweg 145 2628 AL Delft T +31 (0)15-2577008 F +31 (0)15-2788842	intespring	Naam: Buis 18x1.5
Getekend door: Freeke van Osch	Datum: 19-10-2010	Schaal: 1:2 A4 Sheet 1 van 1



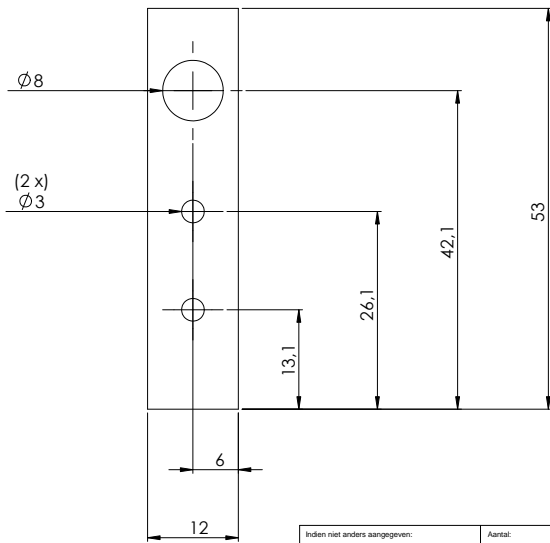
Indien niet anders aangegeven: Toleranties: Afstanden: 0,1 mm Hoeken: 0,5 gr	Aantal: 1	Materiaal: Staal		
	Projectcode: V06.03	Afwerking: <afwerking>		
InteSpring B.V. Rotterdamseweg 145 2628 AL Delft T +31 (0)15-2577008 F +31 (0)15-2788842	intespring	Naam: Buis 35x2 - kopie		
		Getekend door: Freeke van Osch	Datum: 19-10-2010	Schaal: 1:5
2	3	4	5	6

SolidWorks Student License
Academic Use Only



Indien niet anders aangegeven: Toleranties: Afstanden: 0,1 mm Hoeken: 0,5 gr	Aantal: 1	Materiaal: Staal 1 mm		
	Projectcode: V06.03	Afwerking: <afwerking>		
InteSpring B.V. Rotterdamseweg 145 2628 AL Delft T +31 (0)15-2577008 F +31 (0)15-2788842	intespring	Naam: Kabelplaatje - kopie		
		Getekend door: Freeke van Osch	Datum: 19-10-2010	Schaal: 2:1
2	3	4	5	6

SolidWorks Student License
Academic Use Only



Indien niet anders aangegeven: Toleranties: Afstanden: 0,1 mm Hoeken: 0,5 gr	Aantal: 1	Materiaal: Staal 1 mm
	Projectcode: V06.03	Afwerking: <afwerking>
InteSpring B.V. Rotterdamseweg 145 2628 AL Delft T +31 (0)15-2577008 F +31 (0)15-2788842	intespring	Naam: Kabelplaatje
		Getekend door: Freeke van Osch
	Schaal: 2:1	A4
		Sheet 1 van 1

SolidWorks Student License
Academic Use Only

2

3

4

5

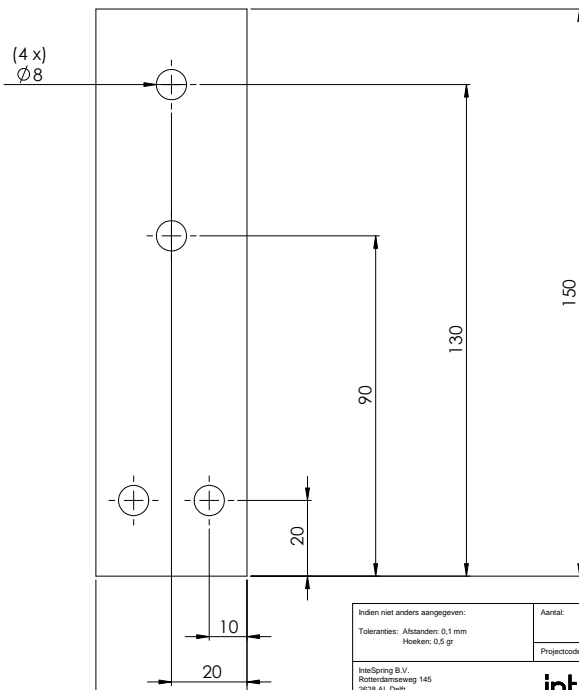
6

A

B

C

D



Indien niet anders aangegeven: Toleranties: Afstanden: 0,1 mm Hoeken: 0,5 gr	Aantal: 3	Materiaal: Staal
	Projectcode: V06.03	Afwerking: <afwerking>
InteSpring B.V. Rotterdamseweg 145 2628 AL Delft T +31 (0)15-2577008 F +31 (0)15-2788842	intespring	Naam: Platstaf 40x10 - kopie (2)
		Getekend door: Freeke van Osch
	Schaal: 1:1	A4
		Sheet 1 van 1

SolidWorks Student License
Academic Use Only

2

3

4

5

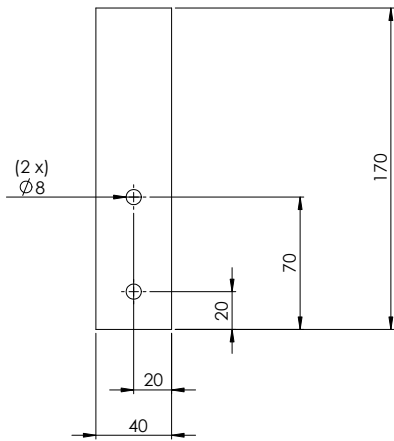
6

A

B

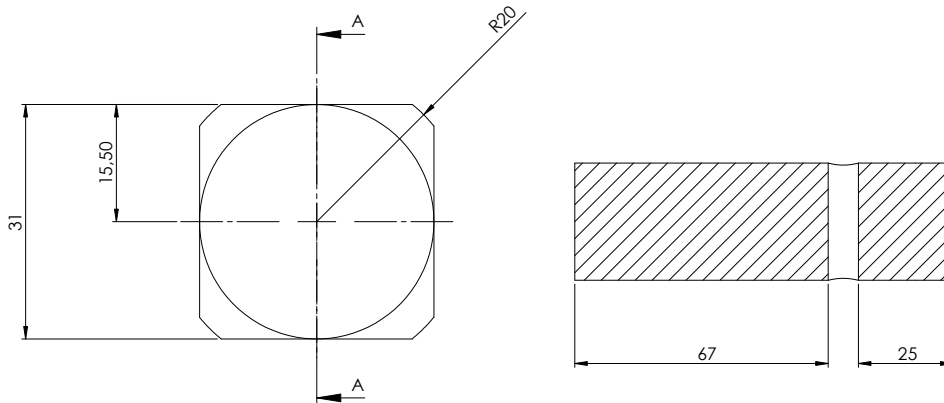
C

D



Indien niet anders aangegeven: Toleranties: Afstanden: 0,1 mm Hoeken: 0,5 gr	Aantal: 2	Materiaal: Staal
	Projectcode: V06.03	Afwerking: <afwerking>
InteSpring B.V. Rotterdamseweg 145 2628 AL Delft T +31 (0)15-2577008 F +31 (0)15-2788842	intespring	Naam: Platstaf 40x10 - kopie (4)
		Getekend door: Frieke van Osch
Datum: 19-10-2010	Schaal: 1:2	A4
	5	6

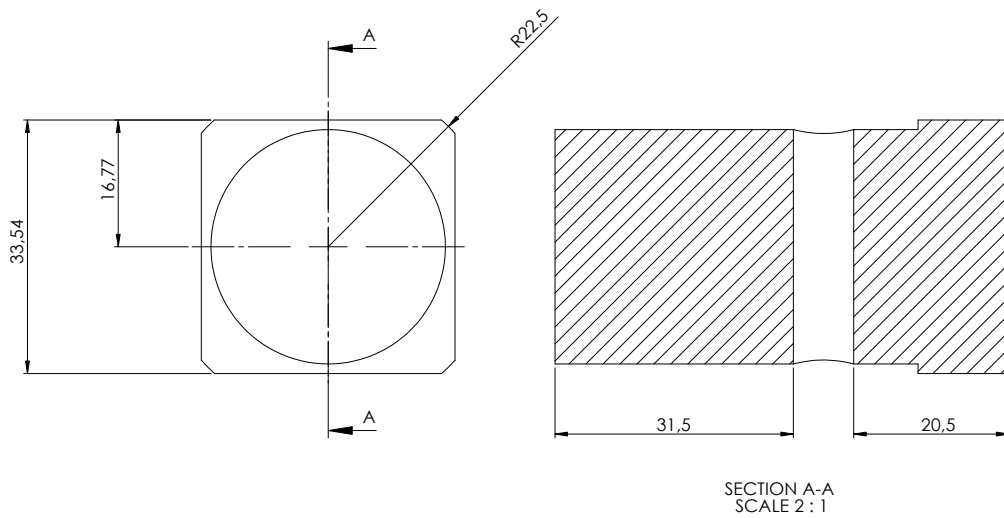
SolidWorks Student License
Academic Use Only



SECTION A-A
SCALE 1 : 1

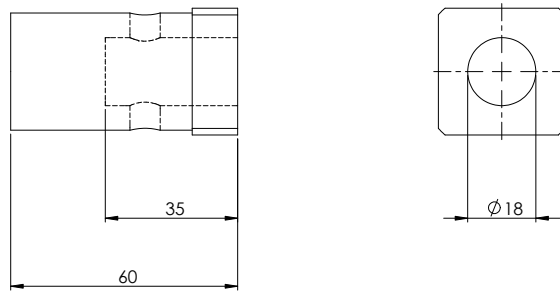
Indien niet anders aangegeven: Toleranties: Afstanden: 0,1 mm Hoeken: 0,5 gr	Aantal: <aantal>	Materiaal: <materiaal>
	Projectcode: <code>	Afwerking: <afwerking>
InteSpring B.V. Rotterdamseweg 145 2628 AL Delft T +31 (0)15-2577008 F +31 (0)15-2788842	intespring	Naam: Prop - kopie (3)
		Getekend door: Mike Hüscher
Datum: 19-10-2010	Schaal: 2:1	A4
	5	6

SolidWorks Student License
Academic Use Only



SolidWorks Student License
Academic Use Only

Indien niet anders aangegeven: Toleranties: Afstanden: 0,1 mm Hoeken: 0,5 gr	Aantal: 1	Materiaal: Staal
	Projectcode: V06.03	Afwerking: <afwerking>
InteSpring B.V. Rotterdamseweg 145 2628 AL Delft T +31 (0)15-2577008 F +31 (0)15-2788842	intespring	Naam: Prop - kopie (4)
Getekend door: Freeke van Osch	Datum: 19-10-2010	Schaal: 2:1
2	3	4
		5
		6



SolidWorks Student License
Academic Use Only

Indien niet anders aangegeven: Toleranties: Afstanden: 0,1 mm Hoeken: 0,5 gr	Aantal: 1	Materiaal: Staal
	Projectcode: V06.03	Afwerking: <afwerking>
InteSpring B.V. Rotterdamseweg 145 2628 AL Delft T +31 (0)15-2577008 F +31 (0)15-2788842	intespring	Naam: Prop - kopie (5)
Getekend door: Freeke van Osch	Datum: 19-10-2010	Schaal: 1:1
2	3	4
		5
		6

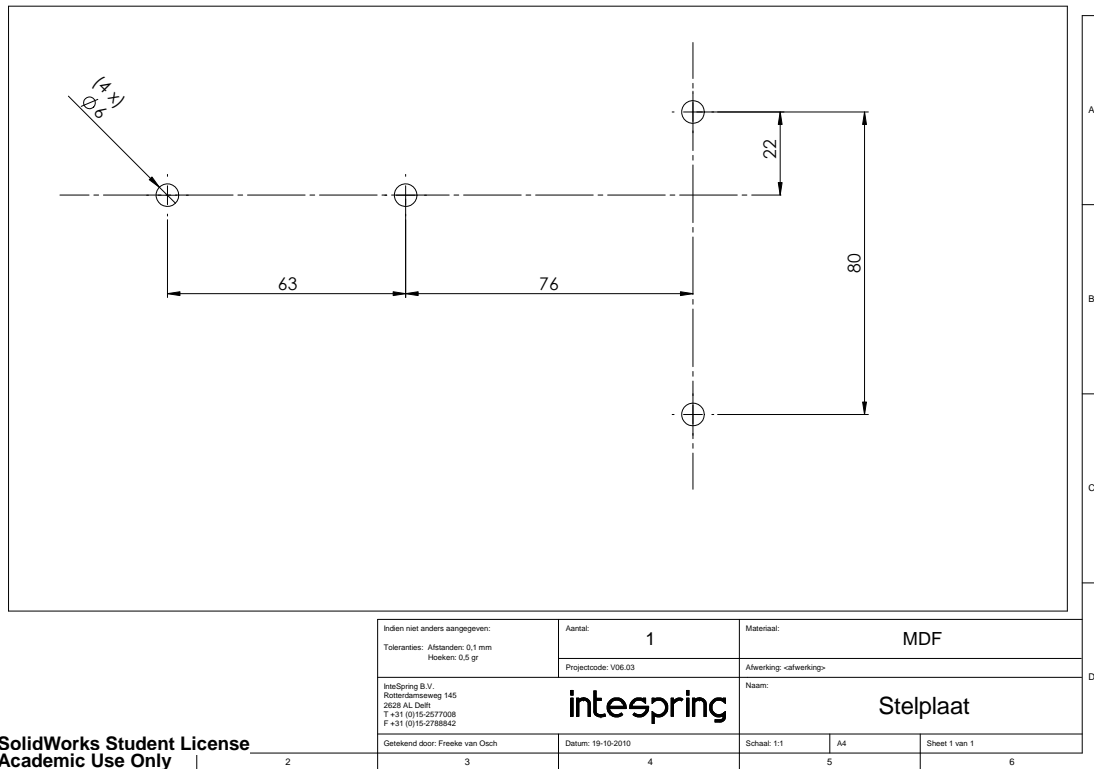
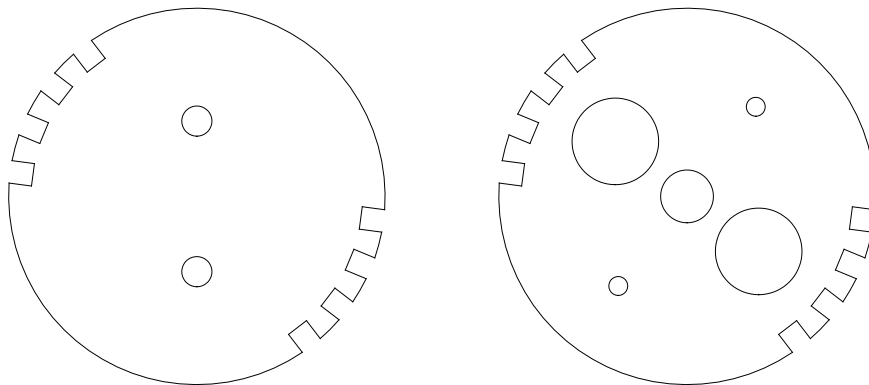


Figure D.4: Drawings of general parts of the prototype

D.2.2 Laser cutting



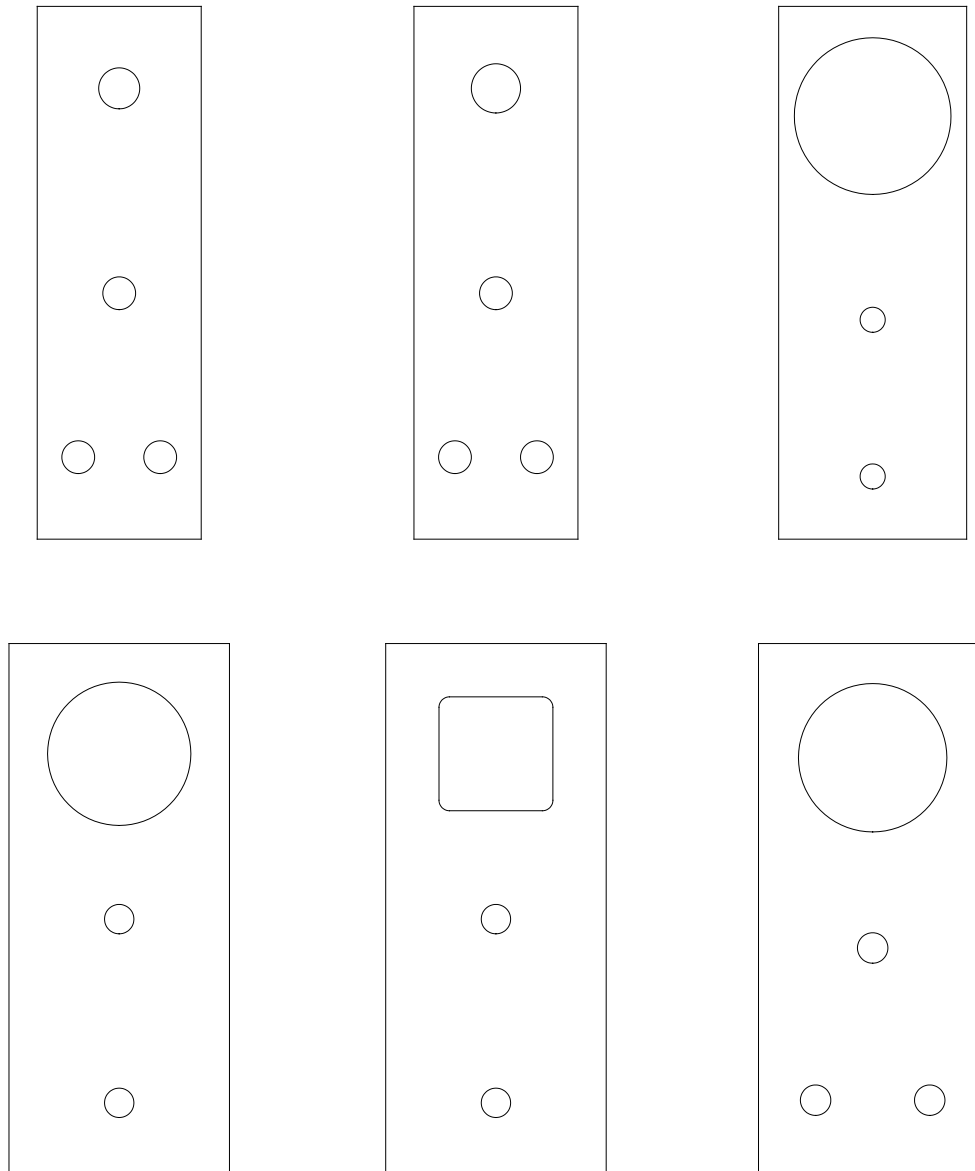


Figure D.5: Drawings of laser cutting parts of the prototype

D.3 List of suppliers

All ordered materials and their suppliers are listed in Tab. D.4 below.

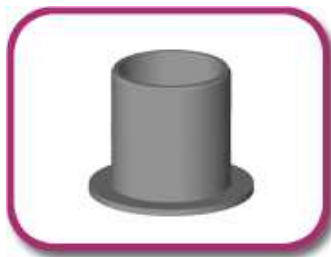
Table D.4: List of suppliers

Part(s)	Supplier
Torsion bars	United Springs (http://www.united-springs.nl)
Cams (rapid prototyping)	Materialise (http://www.materialise.com/online-rapid-prototyping)
Cable	Carl Stahl Benelux B.V. (http://www.carlstahl.nl)
Sheetmetal (laser cutting)	247Tailorsteel (http://www.247tailorsteel.com)
Radial ball bearings	Conrad (http://www.conrad.nl)
Slide bearings	Skiffy (http://www.skiffy.com)

D.4 Specifications of slide bearings

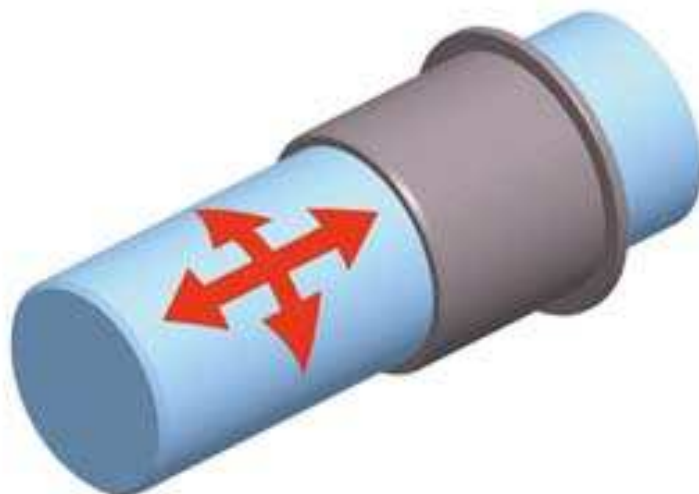


GLIJLAGER SERIE 008-2

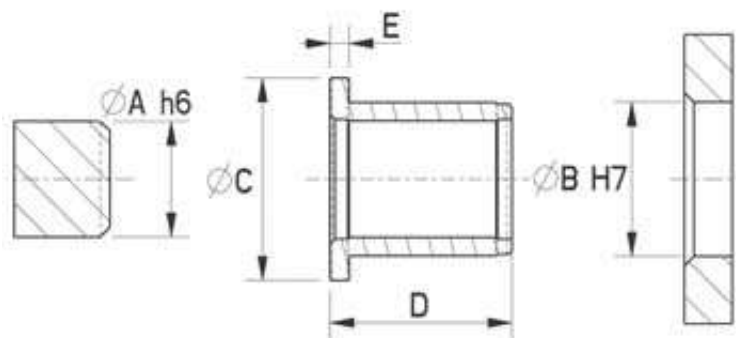


- Gemaakt van speciale nylon-66 (PA-66) compound met carbonvezel en PTFE
- Beschikbare kleuren: zwart
- Zeer lage wrijving en goede warmteafvoer
- Maximale glijnsnelheid roterend 0,9 m/s
- Wrijfingscoëfficiënt t.o.v. staal 0,11 (statisch)
- Lagerhuis H7 tolerantie, as h6

Gebruiks- voorbeelden



Maten



Maten in mm

Maten in inches

Prijzen in Euro

Art. nummer	Kleur	A	B	C	D	E	F	Prijs	Per	Prijs	Per	Prijs	Per
008 7050 114 42	■	6.0	8.0	12.0	4.0	1.0		240.78	1000	149.89	500	39.13	100
008 7070 114 42	■	6.0	8.0	12.0	6.0	1.0		245.80	1000	153.01	500	39.94	100
008 7090 114 42	■	6.0	8.0	12.0	8.0	1.0		250.81	1000	156.13	500	40.76	100
008 7110 114 42	■	6.0	8.0	12.0	10.0	1.0		255.83	1000	159.26	500	41.57	100
008 7130 114 42	■	8.0	10.0	15.0	5.5	1.0		270.88	1000	168.62	500	44.02	100
008 7150 114 42	■	8.0	10.0	15.0	7.5	1.0		275.90	1000	164.85	500	43.45	100
008 7170 114 42	■	8.0	10.0	15.0	10.0	1.0		285.93	1000	170.84	500	45.03	100
008 7190 114 42	■	8.0	10.0	15.0	15.0	1.0		300.98	1000	179.83	500	47.40	100

Appendix E

Measurement setup

The measurements were carried out with a M250-2.5 CT universal testing machine of Testometric (see Fig. E.1). The specifications of this machine are shown in Tab. E.1.



Figure E.1: M250-2.5 CT universal testing machine of Testometric

Table E.1: Specifications of the M250-2.5 CT universal testing machine of Testometric

Description	Specification
Machine capacity	2.5 kN
Speed range	0.001 to 1000 mm/min (in steps of 0.001 mm/min)
Crosshead travel (excluding grips)	1000 mm
Throat	200 mm

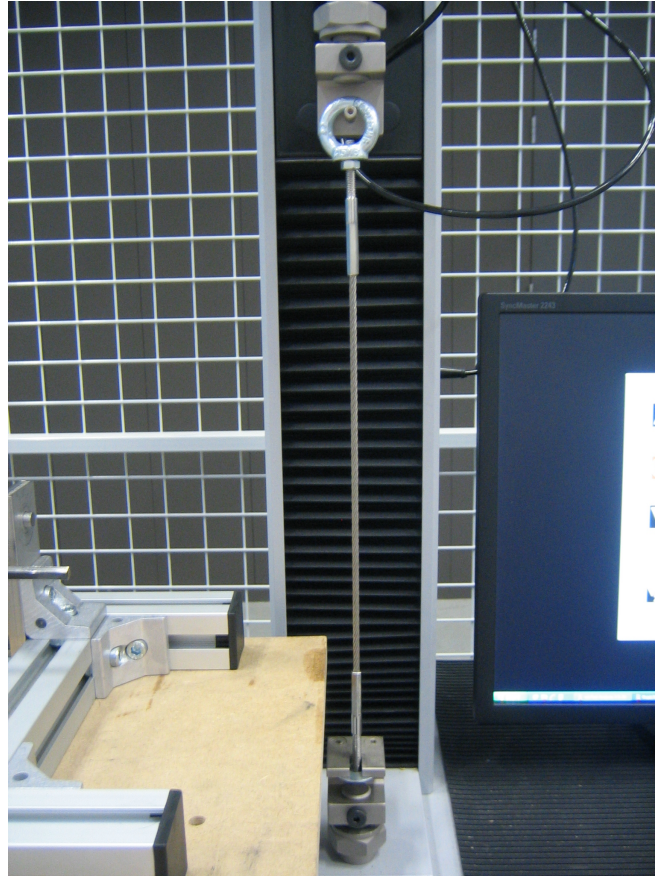


Figure E.2: Measurement setup for the cable of the DCT in the universal testing machine

The first measurements were done with the stainless steel cable of the DCT. The cable was fixed in between the two grippers of the universal testing machine (see Fig. E.2). Three consecutive measurements were done, of which the results are shown in the paper.

Next, several measurements on the prototype were done. A schematic overview of the measurement setup is shown in Fig. E.3. The axes of the testing disc (point D), is connected to the axes of cam 1 of the prototype, with a tube. The tube is fixed on both axis and therefore the rotation of the testing disc is the same as the rotation of cam 1. Since the force in the testing cable is measured and the radius of the testing disc is known, the exerted moment on cam 1 can be calculated. A picture of the measurement setup with the prototype is shown in Fig. E.4.

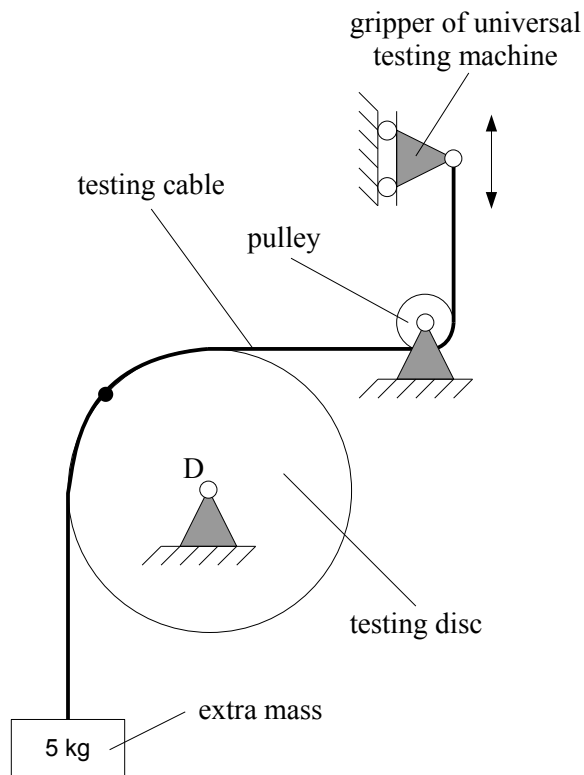


Figure E.3: Schematic representation of the measurement setup for the prototype

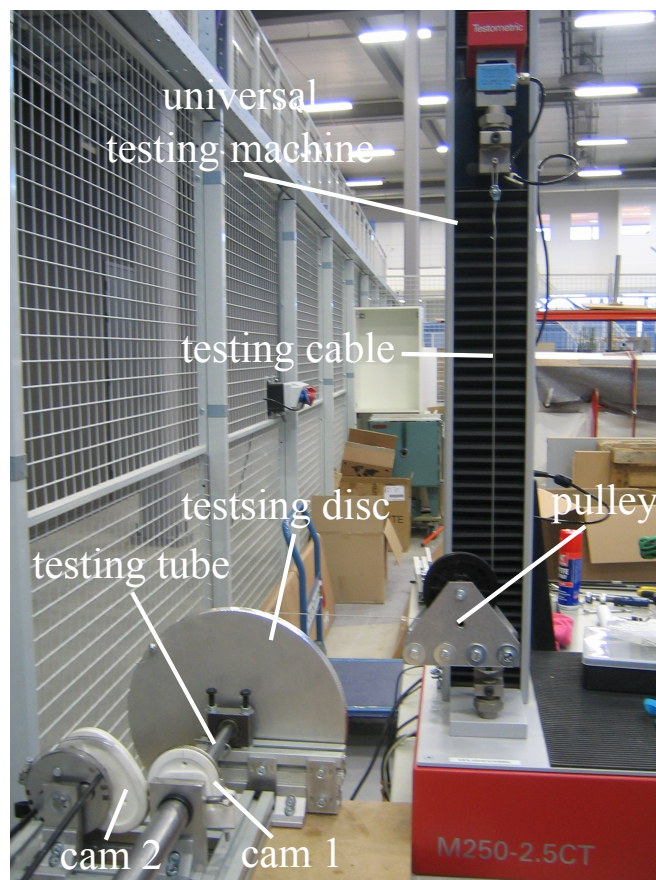


Figure E.4: The measurement setup for the prototype with the universal testing machine

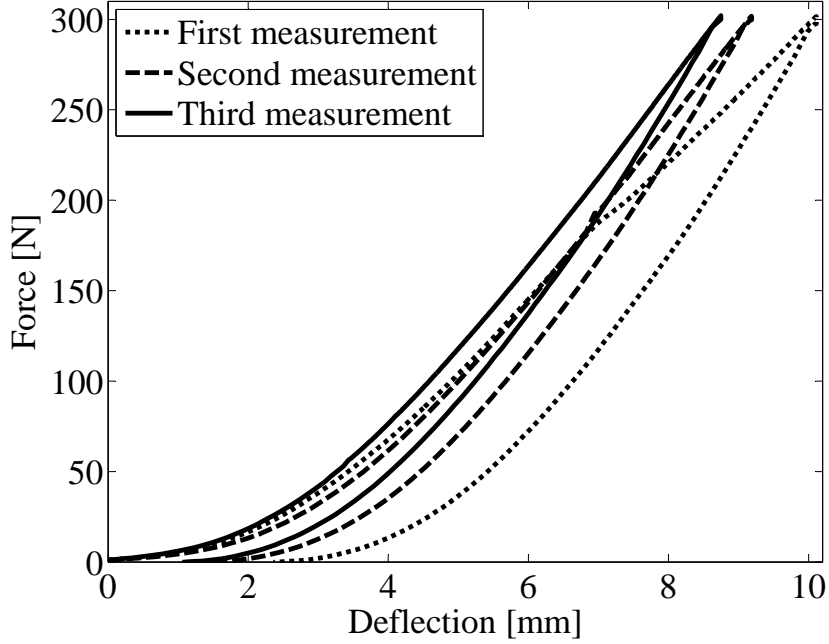


Figure E.5: Three consecutive measurements of the testing cable with the universal testing machine

An extra mass of 5 kg was attached to the testing disc. In this way the testing cable was already stretched at the beginning of the measurements, which avoids the relatively high strain of the cable at the beginning (see Fig. E.5). The measurements shown in the paper are compensated already for this extra mass.

The connection between the testing disc and cam 1, the testing tube, is assumed to be rigid. However, actually the stiffness of the testing tube should be taken into account too. The moments on the system are maximal when $\alpha = \frac{\pi}{2}$ rad. The maximum moment measured can be seen from Fig. 9 of the paper and is 30.7 Nm. The extra mass of 5 kg, attached to the testing disc, adds an extra moment of $5 \cdot 9.81 \cdot 0.15 = 7.4$ Nm (the radius of the testing disc is 150 mm). The maximum total moment on the system is:

$$M_{mass}\left(\frac{\pi}{2}\right) = 30.7 + 7.4 = 38 \text{ Nm}$$

The stiffness of the testing tube is equal to $2.7 \cdot 10^3$ Nm/rad. The angle of rotation α^* of the tube, due to M_{mass} , is:

$$\alpha^* = \frac{38}{2.7 \cdot 10^3} = 0.014 \text{ rad}$$

Since this error is $< 1 \%$, it is assumed that the connection between the testing disc and cam 1 is rigid.

The measurements in the paper were carried out with $\beta_0 = 0.5$ rad. The same measurements can be done with $\beta_0 = 0$ rad, as originally intended (see Fig. E.6). It is clear to see that in this case the operation of the DCT is different at the beginning of the measurements.

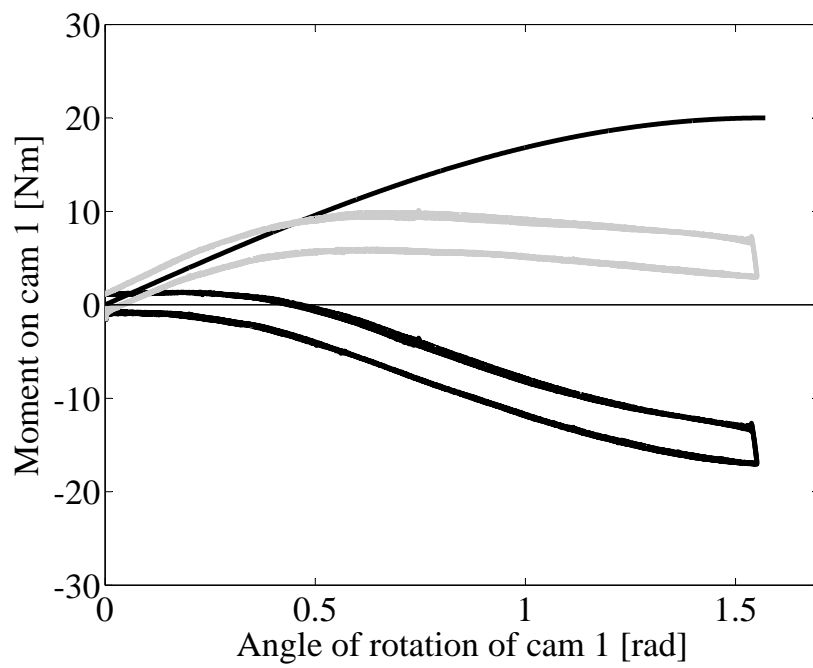


Figure E.6: Three consecutive measurements on cam 1 of M_{bars} , with $n = 2$ and $l = 710$ mm. M_{mass} is the calculated theoretical value.

Appendix F

MATLAB code

F.1 Prototype: centrodes of cams and number, length and width of torsion bars

```
1 % Deze mfile berekent de vorm van beide rolling links. De curve wordt in
2 % X,Y,Z coördinaten opgeslagen in twee .txt bestanden genaamd schijf1.txt
3 % en schijf2.txt. Vervolgens wordt een matrix T weergegeven waarin de
4 % mogelijkheden voor het torsiestaafcluster staan.
5
6 close all
7 clear
8 clc
9
10 %%%%%%%%%%%%%%%%%%%%%%%%%%%%%%%%%%%%%%%%%
11 %% Input %%
12 %%%%%%%%%%%%%%%%%%%%%%%%%%%%%%%%%%%%%%%%%
13
14 m_min = 20;           % Minimale massa [kg]
15 m_max = 30;           % Maximale massa [kg]
16 d_out = 4.00;        % Buitendiameter kabel [mm]
17 AB = 130;            % Afstand tussen de assen van beide schijven [mm]
18 g = 9.81;            % Zwaartekrachtversnelling [m/s^2]
19 L = 0.4;             % Afstand tussen draaipunt en massamiddelpunt [m]
20 T = 2;               % Transmissie tussen beide schijven [-]
21 b_min = 1;           % Minimale breedte torsiestaven [mm]
22 b_max = 10;          % Maximale breedte torsiestaven [mm]
23 n_max = 10;          % Maximaal aantal torsiestaven [-]
24 l_max = 1;           % Maximale lengte torsiestaven [m]
25 G = 78e9;            % Schuifmodulus [Pa]
26 tau_max = 850e6*0.8; % Maximale schuifspanning (met veiligheidsfactor) [Pa]
27 StepSize = 0.001;   % Precisie van de berekening [rad]
28
29 %%%%%%%%%%%%%%%%%%%%%%%%%%%%%%%%%%%%%%%%%
30 %% Berekeningen rollings links %%
31 %%%%%%%%%%%%%%%%%%%%%%%%%%%%%%%%%%%%%%%%%
32
33 % Ruimte voor de rolling links [mm]
34 X = AB-d_out;
35 % Hoekverdraaiing van de schijf aan de massa [rad]
36 alpha = 0:StepSize:pi/2;
37 % Hoekverdraaiing van de schijf aan de torsiestaven [rad]
38 beta = 2/T*sqrt(1-cos(alpha));
39 % Straal van de schijf aan de massa [mm]
40 r1 = X*sin(alpha)/(sin(alpha)+T*sqrt(1-cos(alpha)));
41 % Straal van de schijf aan de torsiestaven [mm]
42 r2 = 0.5*X*T^2*beta/(0.5*T^2*beta+sin(acos(1-T^2*beta.^2/4)));
43 % Minimale schijfheid van het torsiestaafcluster [Nm/rad]
44 k_min = 0.5*m_min*g*L*T^2;
45 % Maximale schijfheid van het torsiestaafcluster [Nm/rad]
46 k_max = 0.5*m_max*g*L*T^2;
47
48 %%%%%%%%%%%%%%%%%%%%%%%%%%%%%%%%%%%%%%%%%
```

```

49  %%% Berekeningen torsiestaaflcluster %%%
50  %%%%%%%%%%%%%%%%%%%%%%%%%%%%%%%%%%%%%%%%%%%%%%%%%%%%%%%%%%%%%%%%%%%%%%%%%
51
52  j = 0; % aantal mogelijke oplossingen
53  S = 0; % matrix met alle mogelijke oplossingen
54
55  for i = 1 : (b_max-b_min)+1 % aantal mogelijke breedtes van de torsiestaven [-]
56      b = (b_min + (i-1)) / 1000; % elke mogelijke breedte van de torsiestaven
57      for n = 1 : n_max % aantal mogelijkheden voor de hoeveelheid staven [-]
58          l_1 = 0.1406*G*b^4/(k_min/n); % lengte torsiestaven bij minimale massa [m]
59          l_2 = 0.1406*G*b^4/(k_max/n); % lengte torsiestaven bij maximale massa [m]
60          b_max = 1.482*tau_max*l_2/(max(beta)*G); % breedte bepaald door kortste lengte [m]
61          % De lengte van de torsiestaven moet korter zijn dan de maximale
62          % opgegeven lengte door de gebruiker. Tevens mag de breedte niet
63          % groter zijn dan de berekende maximaal toelaatbare breedte.
64          if l_1 < l_max & b < b_max
65              % Het aantal mogelijke oplossingen neemt met 1 toe.
66              j = j+1;
67              % De eerste kolom van de oplossingsmatrix bevat de lengte van
68              % de torsiestaven.
69              S(j,1) = l_1;
70              % De tweede kolom van de oplossingsmatrix bevat de breedte van
71              % de vierkante torsiestaven.
72              S(j,2) = b;
73              % De derde kolom van de oplossingsmatrix bevat het aantal
74              % staven in het torsiestaaflcluster.
75              S(j,3) = n;
76          end
77      end
78  end
79
80  % Laat alle mogelijke oplossingen voor het cluster zien.
81  disp('    LENGTE    BREEDTE    AANTAL')
82  disp(S)
83
84  %%%%%%%%%%%%%%%%%%%%%%%%%%%%%%%%%%%%%%%%%%%%%%%%%%%%%%%%%%%%%%%%%%%%%%%%%
85  %%% Plots %%%
86  %%%%%%%%%%%%%%%%%%%%%%%%%%%%%%%%%%%%%%%%%%%%%%%%%%%%%%%%%%%%%%%%%%%%%%%%%
87
88  polar(alpha,r1,'r');
89  title('Schijf aan massa')
90  figure
91  polar(beta,r2,'r');
92  title('Schijf aan torsiestaven')
93
94  %%%%%%%%%%%%%%%%%%%%%%%%%%%%%%%%%%%%%%%%%%%%%%%%%%%%%%%%%%%%%%%%%%%%%%%%%
95  %%% Output %%%
96  %%%%%%%%%%%%%%%%%%%%%%%%%%%%%%%%%%%%%%%%%%%%%%%%%%%%%%%%%%%%%%%%%%%%%%%%%
97
98  [X1,Y1] = pol2cart(alpha,r1); % vectoren met cartesische coördinaten voor schijf 1
99  [X2,Y2] = pol2cart(beta,r2); % vectoren met cartesische coördinaten voor schijf 2
100
101  % Sla de vectoren met cartesische coördinaten op in textfiles genaamd
102  % schijf1.txt en schijf2.txt.
103  fid1 = fopen('schijf1.txt','wt');
104  fid2 = fopen('schijf2.txt','wt');
105  for j = 1:length(X1)
106      fprintf(fid1,'%f \t %f \t %d \n',X1(j),Y1(j),0);
107      fprintf(fid2,'%f \t %f \t %d \n',X2(j),Y2(j),0);
108  end
109  fclose(fid1);
110  fclose(fid2);
111
112  % Bereken de booglengte y van de curves
113  y = 0;
114  for i = 2:1570
115      afstand = (beta(i+1)-beta(i))*r2(i+1);
116      y = y + afstand;
117  end
118  y
119  y = 0;
120  for i = 2:1570
121      afstand = (alpha(i+1)-alpha(i))*r1(i+1);

```

```

122     y = y + afstand;
123 end
124 y

```

F.2 Band: thickness, width and minimum required radius

```

1  % Deze mfile geeft voor verschillende bandbreedtes de bijbehorende minimale
2  % straal en banddikte.
3
4  close all
5  clear
6  clc
7
8  %%%%%%%%%%%%%%%%%%%%%%%%%%%%%%%%%%%%%%%%%%
9  %%% Gegevens Systeem %%%
10 %%%%%%%%%%%%%%%%%%%%%%%%%%%%%%%%%%%%%%%%%%
11
12 m_max = 40;           % Maximale massa [kg]
13 g = 9.81;           % Zwaartekrachtversnelling [m/s^2]
14 L = 0.4;           % Afstand tussen draaipunt en massamiddelpunt [m]
15 M = m_max*g*L;     % Maximaal moment op de eerste schijf bij 90 graden [Nm]
16
17 %%%%%%%%%%%%%%%%%%%%%%%%%%%%%%%%%%%%%%%%%%
18 %%% Gegevens Band %%%
19 %%%%%%%%%%%%%%%%%%%%%%%%%%%%%%%%%%%%%%%%%%
20
21 b = 0.01:0.001:0.2; % Bandbreedte [m]
22 t = 0.1e-3:0.1e-3:1e-3; % Banddikte [m]
23
24 %%%%%%%%%%%%%%%%%%%%%%%%%%%%%%%%%%%%%%%%%%
25 %%% Materiaalconstanten %%%
26 %%%%%%%%%%%%%%%%%%%%%%%%%%%%%%%%%%%%%%%%%%
27
28 sigma_y = 0.8*1400e6; % Vloei grens [Pa]
29 E = 210e9;           % Elasticiteitsmodulus [Pa]
30
31 %%%%%%%%%%%%%%%%%%%%%%%%%%%%%%%%%%%%%%%%%%
32 %%% Berekeningen %%%
33 %%%%%%%%%%%%%%%%%%%%%%%%%%%%%%%%%%%%%%%%%%
34
35 % Voor verschillende waarden van de bandbreedte wordt de bijbehorende
36 % minimale straal en de daarbijhorende banddikte berekend. Deze oplossingen
37 % worden opgeslagen in de matrix S.
38 for i = 1:length(b) % Voor iedere opgegeven waarde van de bandbreedte uitvoeren.
39     r = (0.5*E*t+M./(t*b(i)))/sigma_y; % De straal wordt berekend vanuit banddikte.
40     r_min = min(r); % De minimale straal is de kleinste waarde uit de vector r.
41     [I,J] = find(r == r_min); % Vindt de plaats van r_min in de vector r.
42     S(i,1) = b(i); % Plaats de bandbreedte in de eerste kolom van matrix S.
43     S(i,2) = t(J); % Plaats de banddikte (behorende bij r_min) in de tweede kolom.
44     S(i,3) = r_min; % Plaats de minimale straal in de derde kolom.
45 end
46
47 %%%%%%%%%%%%%%%%%%%%%%%%%%%%%%%%%%%%%%%%%%
48 %%% Output %%%
49 %%%%%%%%%%%%%%%%%%%%%%%%%%%%%%%%%%%%%%%%%%
50
51 disp('   Breedte   Dikte   Straal')
52 disp(S)

```